Tree-root anchorage:

Stability of trees based on real tree-root architecture

Johnatan Ramos Rivera

Anclaje árbol-raíz:
Estabilidad de árboles basado en la arquitectura real del sistema árbol-raíz.

UNIVERSIDAD
NACIONAL
DE COLOMBIA

Tree-root anchorage: stability of trees based on real tree-root architecture

Anclaje árbol-raíz: Estabilidad de árboles basado en la arquitectura real del sistema árbol-raíz.

Johnatan Ramos Rivera

Universidad Nacional de Colombia

Facultad de minas, Departamento de Ingeniería Civil

Medellín, Colombia

2019

Tree-root anchorage: stability of trees based on real tree-root architecture

Anclaje árbol-raíz: Estabilidad de árboles basado en la arquitectura real del sistema árbol-raíz.

Johnatan Ramos Rivera

Tesis presentada como requisito parcial para optar al título de:

MSc en Geotecnia

Director (a):

Msc. Oscar Echeverri Ramírez

Línea de Investigación:

Ingeniería Geotécnica

Grupo de Investigación:

Grupo de investigación en Geotecnia

Universidad Nacional de Colombia

Facultad de minas, Departamento de Ingeniería Civil

Medellín, Colombia

2019

I dedicate this thesis to my family and beloved wife; I couldn't have done this without them. Thank you for all their support along the way.

This journey also taught me that the highest purpose and happiness in my life will always be the result of doing what I love.

Acknowledgements

I have learned a lot and really enjoyed while working on this thesis, It made me to remember all my colleagues and

I consider myself fortunate indeed to have had the opportunity to pursue my master's degree with Professor Oscar Echeverri-Ramirez who encourage me since my bachelor's degree to continue working with him and for his invaluable guidance, vision and sincerity though my academic and personal life. I would also like to thank him for his friendship, empathy and valuable advices.

I would like to take this opportunity to express my deep gratitude to my supervisor Professor Harianto Rahardjo for his support, advice, motivation and mainly to believe and trust in me to carried out my research in Singapore. Special and deeply thanks also to Dr. Daryl Lee Tsen-Tieng for his counselling and to be an example of the success is gained by sharing knowledge not by keeping it and to always have time to share a cup of coffee and talk of a better tomorrow.

I would also like to express my appreciation to the Singapore National Parks Board (NParks) for the research funding who helped me to arrive to Singapore. The contribution of the Nanyang Technological University through Nanyang Environmental and Water Research Institute (NEWRI), Environmental Processes Modelling Centre (EPMC) in terms of manpower funding and assistance is also greatly appreciated. Thanks, are also extended to Dr. Fong Yok King of NParks.

Abstract

Climate change impact on tree stability is often associated with higher risk of wind-throw due to higher frequency and magnitudes of the extremes of climate. Higher lateral loads due to increase in maximum wind and rainfall reduces tree anchorage due to a decrease in soil matric suction and consequently the overall strength in trunk-root-soil.

This study made comparisons of the mechanical response of trees with different root architectures using static loading test conducted in the field and numerical analysis of laser-scanned root systems. For this case, *Samanea saman*, *Khaya senegalensis* and *Syzygium grande* were the tree species selected and analysed.

The tree-root system models consisted of root system architectures obtained using 3D-laser scanning. A parametric analysis was conducted by varying the modulus of elasticity of the soil (E_s) from 2.5 to 25 MPa and the results were compared with the static load tests to obtain the overall mechanical responses of the soil-tree root systems.

The results showed important dependencies of the mechanical responses of the soil-tree root with the lateral load magnitudes with respect to the root architecture. The numerical models were also able to estimate the effective leeward and windward anchorage zones with different soil elastic modulus and rooting architectures to define the Tree Protection Zone (TPZ).

Keywords: Tree stability, numerical modeling, static loading test, soil-tree rooting system.

Table of Content

Page.

1. INTRODUCTION 3
1.1 Research background 3
1.2 Aims & objectives 4
1.2.1 General 5
1.2.2 Specific 5
1.3 Scope and limitations 5
1.4 References 6

2. BACKGROUND 7
2.1 Introduction 7
2.2 Elements and phenomena involved in tree stability 7
2.3 Tree-roots and stability 8
2.4 Antecedents 12
2.4.1 Singapore environment 12
2.4.2 Colombian environment 12
2.5 Structural analysis of trees 14
2.5.1 Slope-deflection equations 15
2.6 Static tree pulling test 16
2.7 Resisting moments of trees under static loading 17
2.8 Numerical Simulations 19
2.8.1 Saturated soil media 20
2.9 References 20

3. RESEARCH PROGRAM-METHODOLOGY 24
3.1 Introduction 24
3.2 Site and tree selection 25
3.3 Soil sampling and testing 27
3.3.1 Tree survey characteristics 27
3.4 Static loading test 28
3.5 Air spading 30
3.6 Laser scanning of tree-root system 30
3.7 Numerical modelling and verification 31
3.7.1 Simulation set-up 32
3.8 References 34

4. RESULTS 37
4.1 Tree-root geometry and root architecture 37

4.2 Static loading test 39
4.2.1 Sensitivity of individual trees under lateral force 39
4.3 Numerical modelling 42
4.3.1 Parametric analysis 43
4.4 M–α response curves: comparison in-situ behaviour and simulation measurements 46
4.5 Estimation of structural root protection zone based on actual rooting architecture 47
4.6 References 49

5. CONCLUSION AND REMARKS 51
5.1 Overall conclusion 51
5.2 Specific Conclusions 51
5.3 Future studies 52

6. APPENDIX 53

List of Figures

Page.

Figure 2-1 Mechanical stability of trees associated to strong winds (Quine, 1995) 8
Figure 2-2 Left: Tree failure at Fourth Ave (2014),. Right: Tree failure at Pasir Ris, Singapore (2012); adopted from Rahardjo et al 2016 9
Figure 2-3 Types of roots in the rooting system of common tree species. (Costello et al., 2011) ... 10
Figure 2-4 Shallow-rooted tree explaining the four components of the anchorage which resist overturning or bending moments (adapted from Coutts, 1983) 10
Figure 2-5 Schematic of a mature tree root system with secondary sinkers' when laterally loaded to the right by wind (guying zone has practically no moment arm to the hinge) (Danjon et al., 2009) 11
Figure 2-6 Singapore Botanical Garden accident caused by tree failure. 12
Figure 2-7 Tree failure on Calazans neighbourhood due to high rainfall intensity on 11th March/2019 leave several damages to infrastructure. 13
Figure 2-8 Tree collapse accident took the life of a civilian from Cucuta city in Sardinata Roadway on 23rd April/2019 13
Figure 2-9 Tree uprooting caused several damages to local housing in Cartagena and two habitants got injured during the rainfall of 7th June/2019. 13
Figure 2-10 Slope-Deflection Equation for cantilever beam 15
Figure 2-11 Combined resisting moment as a function of leaning angle from a typical tree pulling test experiments. (England et al, 2000) 17
Figure 2-12 Static tree pull results. Maximum overturning moment is 350 kN.m. all related to equation ($H.DBH^2$) to predict stability and failure (from Cucchi et al., 2004) 18
Figure 2-13 Stem failure was seen in 29 out of 164 Pinus radiata in NZ. The maximum stem failure resistive bending moments (kN.m) were compared to the theorical values calculated (from Moore, 2000). 19
Figure 3-1 Outline research program 25
Figure 3-2 Study area within the geological map of Singapore (Adapted from DSTA, 2009) 26
Figure 3-3 Selected trees at Changi Village, (a) *Syzygium grande*, (b) *Khaya senegalensis*, (c) *Samanea Saman* 26
Figure 3-4 Static pull test a) Setup for the static loading test b) capstan winch and winching point of test tree 29
Figure 3-5 (a) exposed root plate of the air spaded *S. grande.* (b): Lifted exposed root plate of the air spaded *K. senegalensis* in preparation for laser scanning. 30
Figure 3-6 REIGL VZ-400 terrestrial scanner with the attached top mounted NIKON full frame camera used in this investigation 31
Figure 3-7 Numerical model domain and border conditions. 32
Figure 3-8 Bonded contact interface in *S. Saman* tree. 33

Figure 3-9 Bonded contact interface in *K. Senegalensis* tree..... 34
Figure 4-1 Root architecture K. senegalensis (a) Plan view, (b) front view. 37
Figure 4-2 Root architecture *S. saman* (a) Plan view, (b) front view. 38
Figure 4-3 Root architecture *S. grande* (a) Plan view, (b) front view..... 38
Figure 4-4 Lateral force versus lateral deflection response, a) *K. senegalensis* (KS), b) *S. saman* (SS), c) *S. grande* (SG) 40
Figure 4-5 Static Loading Test results a) K. senegalensis (KS). 41
Figure 4-6 Static Loading Test results *S. saman* (SS*)*. 41
Figure 4-7 Static Loading Test results *S. grande* (SG). 42
Figure 4-8 Overall stresses of the K. senegalensis tree varying elastic modulus of the soil [(a)-Es= 2.5 MPa, (b)- Es= 5.0 MPa, (c)- Es= 10.0 MPa, (d)- Es= 25.0 MPa]..... 44
Figure 4-9 Overall stresses of the S. saman tree varying elastic modulus of the soil (a)-Es= 2.5 MPa, (b)- Es= 5.0 MPa, (c)- Es= 10.0 MPa, (d)- Es= 25.0 MPa..... 45
Figure 4-10 Comparison experimental and predicted model, a) *K. senegalensis* (KS), b) *S. saman* (SS). 46
Figure 4-11 Stress contours due to lateral load on root architecture a,b) *K. senegalensis*, c,d) *S. saman*. 49

Lista of tables

Page.

Table 3-1 Soil index properties at Changi Villagr 27
Table 3-2 Geometrical characteristics tree species tested. 28
Table 3-3 Mechanical properties tree species 28
Table 3-4 Steps involved in the bending mechanics analysis (Modified from Ludstrom, 2007a) ... 30
Table 4-1 Comparison results obtained from field testing and numerical simulations. 46
Table 6-1 Raw data static pulling test 54
Table 6-2 Numerical analyses varying the soil elastic modulus of the soil from 2.5 MPa to 10 MPa. 54
Table 6-3 Numerical analyses varying the loading location 55

1. INTRODUCTION

1.1 Research background

Trees sway under wind loads. Under light wind conditions, the trunk of the tree hardly deforms; however, large motions can be observed in the branches of the canopy. In some cases, severe wind loads can trigger excessive bending moments that may lead to overall failure. This overall failure can be in the form of breakage of the tree trunk, if the roots are strong enough to resist uprooting or uprooting if the converse is true. The maximum static bending moment resistance of the tree is dictated by three components, a) changes in shear strength of the soil, decay damage or cavities in the tree and c) a complex combination between the bonding of the root and the soil.

In urban areas, individual trees can fail under the influence of high wind loads and cause injury and death to people, damage to property or even both. The "City in a Garden" planning vision of Singapore means that millions of people within a dense urban landscape co-exist in proximity to substantial urban greenery. A large part of this urban greenery comprises of thousands of mature trees that can be found growing along roadsides, in parks and within residential, industrial, shopping and business districts. To ensure a sustainable and harmonious co-existence, a detailed comprehension of the tree biometrics and its response under loads is needed. At present, tree assessments by qualified arborists are based on visual methods like Visual Tree Assessment (VTA) **[Mattheck and Breloer 1994]**.

Visual Tree assessment (VTA) is usually undertaken periodically. When a tree is identified as hazardous (e.g. having structural defects or evidence of decay), more attention is paid to the tree, especially if it is within an area with high pedestrian or vehicular traffic. VTA has been increasingly performed in recent years for both rural and urban areas to realize the objectives of sustainable urban greenery. As the increasing urban populations require more roads, sidewalks, parks and buildings; there will be an exponential increase in the level of interaction between trees and people in a green city. This increase in interaction sometimes can become proportional to the increase in risk. This risk can be mitigated if a considerable effort and attention are made to progress the understanding of tree biomechanics beyond the current VTA practices.

Engineers often use periodical visual inspections of manmade structures to look for cracks and other indicators of structural problems, visual inspections alone are of limited utility and are often associated with subjective judgements and as a result it is possible obtain, slightly different risk assessments of the same tree by different practitioners. Therefore, qualitative and quantitative descriptions using the theories associated with the mechanics of materials can help to standardize

the understanding of tree biomechanics by reducing the complexity of the natural systems through the description of tree structural behaviour as “living structures” using engineering frameworks of stress, deformations and failure criterion, like those created for structural and geotechnical engineering.

The creation of these engineering frameworks to describe tree structural behaviour requires the collection of tree data and development of simplified tree stability models that can describe interactions between the tree-root architectures, material properties, self-canopy wind loads, soil properties and calculate safety factors objectively. These engineering frameworks can assist tree care professionals to use engineering judgement in performing tree care management.

Some of the parameters that influence the potential of wind-throw failure are tree age, geometry, health and local site conditions such as; (i) soil slope angle (ii) soil type, (iii) soil moisture content and (iv) tree species planting density **[Harris et al 1999; Kane 2008]**. Among all these parameters, the governing parameters include the geometry of the tree trunk and the rooting depth as they greatly affect the overall lateral resistance to wind loading as supported by studies conducted by **[Fourcaud et al.,2008, Dupuy et al., 2005, 2007]**.

Soil provides the medium for tree root anchorage and influences root health, because the soil provides the nutrients and water required for tree health and enables photosynthesis. The soil also affects the anchorage depth and the shape of the root system. Increased soil moisture beyond a certain level reduces the attachment or bond between the soil and the roots. As a result, slip surfaces can develop at the contact surfaces between the soil and the roots that can trigger uprooting.

The study of the mechanical response of trees using numerical analysis has been studied by several researchers. However, there is still a lack in the knowledge about the correct estimation of the basic properties and spatial distribution of the biomechanics related to the tree. [**Lee et al, 2018**] presented a closed form solution to understand the commonly occurring shallow root architecture that influences the resistance to uprooting failure. The results allowed the mechanical response of a tree under lateral loading to be simplified and yet remain biomechanically correct by modelling the shallow root-plate system as a shallow footing with multiple lateral roots.

This study attempts to relate the main cause of tree failure represented by the concentrated wind load (**Coutts et al., 1995**) conducting a biomechanical approach in terms of static conditions under real root architecture. **Peltola et al. (2006)** assessed the maximum bending moment for tree failure by pulling tests, working in static conditions.

1.2 Aims & objectives

This thesis contributes to filling the gaps mentioned in the last paragraphs in the following three ways:

(1) Providing relationships for the mechanical response of the main structural elements of the tree, the root-soil system and the trunk;

(2) Assessing the overall mechanical behaviour of the whole tree subject to mechanical stress, originating from static loading.

(3) Investigating to what extension are influenced the structural rooting elements by loads;

Due to the complexity of trees, the approach taken in this study is mainly numerical; experimental test is used to obtain deeper insights into the numerical results and to help to interpret them. To maximize the applicability of the findings, the trees were selected to be representative of Singapore with respect to tree size, species and growth conditions. However, this study also pretends to expand the knowledge of trees in urban environments and replicate it worldwide.

1.2.1 General

This study attempts to use the static loading field test as a potential tool to provide a link between the static loading test results and the structural tree response of the tree-root anchorage system allowing the estimation of the Tree-Root Protection Zone (TRPZ) in terms of stresses and strain.

1.2.2 Specific

This study has been divided in specific objectives in order to achieve the general objective as follows:

- Understand the coupled effect between tree trunk, rooting system and soil media from a static stability perspective based on experimental and numerical simulations.
- Generate a numerical model based on real tree-root architecture from laser scanned geometries and apply load-deformations using a finite element modelling and compare with field test.
- Create a new knowledge from a general basis about the mechanical response of the tree under lateral loads based on Mohr-Coulomb and Von mises failure criteria using real root architecture.
- Give an initial approximation to the estimation of structural tree root protection zone (TRPZ)
- Find the effects of changes in the lateral loading direction regarding the rooting architecture of the scanned trees.
- Propose a preliminary threshold levels in terms of Tree Root Protection Zone (TRPZ) to guarantee global stability of the tree system.

1.3 Scope and limitations

This study presents a comparison between static loading tests conducted on trees and numerical analyses performed on actual rooting geometries within the soil to study the relationships between

the stem-root stresses generated under the application of lateral load under different rooting architectures.

- Pulling test numerical simulations were performed on simplified models of trees that including the existing effects of lean angles.

- Parametric studies of changes in modulus of elasticity of the tree and soil based on pulling test simulation were conducted assuming a Mohr Coulomb behaviour for the soil and V-M behaviour for the tree material.

- Changes in the direction of static loads after calibration were simulated by using point loads to represent wind loads coming from different directions on the trees while parametrically studying the effects of changes in the of modulus of elasticity of the soil.

1.4 References

- Mattheck & Breloer (1994) Field guide for visual tree assessment (VTA), Arboricultural Journal, 18:1, 1-23, DOI: 10.1080/03071375.1994.9746995

- Harris, R. W., Clark, J. R., & Matheny, N. P. (1999). Arboriculture: Integrated management of trees, shrubs and vines, 3rd ed., Englewood Cliffs, NJ: Prentice Hall.

- Kane, B. (2008). “Tree failure following a windstorm in Brewster, Massachusetts, USA.” Urban Forestry and Urban Greening. Urban Forestry & Urban Greening, Volume 7, Issue 1

- Fourcaud, T., Ji, J.N., Zhang, Z.Q., Stokes, A., 2008. Understanding the impact of root morphology on overturning mechanisms: a modelling approach. Ann. Bot. 101, 1267–1280.

- Dupuy L, Fourcaud T, Stokes A. (2005). A numerical investigation into factors affecting the anchorage of roots in tension. European Journal of Soil Sciences. 56:319-327.

- Dupuy L, Fourcaud T, Lac P, Stokes A. (2007). A generic 3D finite element model of tree anchorage integrating soil mechanics and real root system architecture. American Journal of Botany.; P94:1506–1514.

- Lee, D. T. -T., Rahardjo H, Leong EC, Fong YK, (2018). Anchorage and stability of tree root-soil plates, Journal Environmental Geotechnics.

2. BACKGROUND

2.1 Introduction

The structural properties of trees must be determined in order to evaluate their strength and ability to withstand loads under changes in climatic conditions. In urban areas, it is important to assess the risks associated with tree failure to maintain or remove a tree.

The study of trees especially related to tree resilience against climate change has been related to the relationship between the soil, the roots and the climate. This interaction comprises of the cycles of infiltration, seepage and evapotranspiration. These processes play a great role in the trees' structural stability; there have been various studies that have related soil strength to be tree stability against uprooting (**Dupuy et al., 2005a; Fourcaud et al., 2008; Rahardjo et al., 2017**).

According to **Rahardjo et al. (2017)** the interaction between the soil, trees, and the environment involve the complex and simultaneous interaction and variation of many parameters. Any form of climate change (air temperature, relative humidity, solar radiation, precipitation, and wind speed) will change the flux of water into and out of the soil.

The most common expression of climate change in Singapore are in the form of precipitation induced infiltration and other forms of seepage recharge through the movement of water from locations of higher total heads to locations of lower total heads. In some cases, a negative pore water pressure produces a gradual drying, cracking, and desiccation of the soil mass due to increases the soil water balance.

Changes in the soil moisture as described above will also affect the soil structure, soil shear strength and root anchorage. This is because wetter soil tends to have a looser structure. The interactions between the soil and tree roots are without doubt key to tree stability as these interactions are exposed to changes in the environment. **Blight (1997)** describes the interactions that result in changes in the soil water balance.

2.2 Elements and phenomena involved in tree stability

Wind loads associated as a lateral load applied to a tree induce a variety of responses which depend on the magnitude, duration and frequency of loading. Figure 2-1 shows the mechanical stability associated of trees subjected to strong loads (wind) depends on the magnitude of the applied force from the external load acting on the crown and the relative capacity of the stem and root–soil system to resist this applied loading (**Wood 1995; Peltola 2006; Gardiner et al. 2008; Peltola et al. 2013**).

The threshold (or critical) wind speed required to cause uprooting or stem failure can then be defined as the wind speed required to produce an applied bending moment equal to the maximum resistive moment that can be provided by either the stem or the root–soil system.

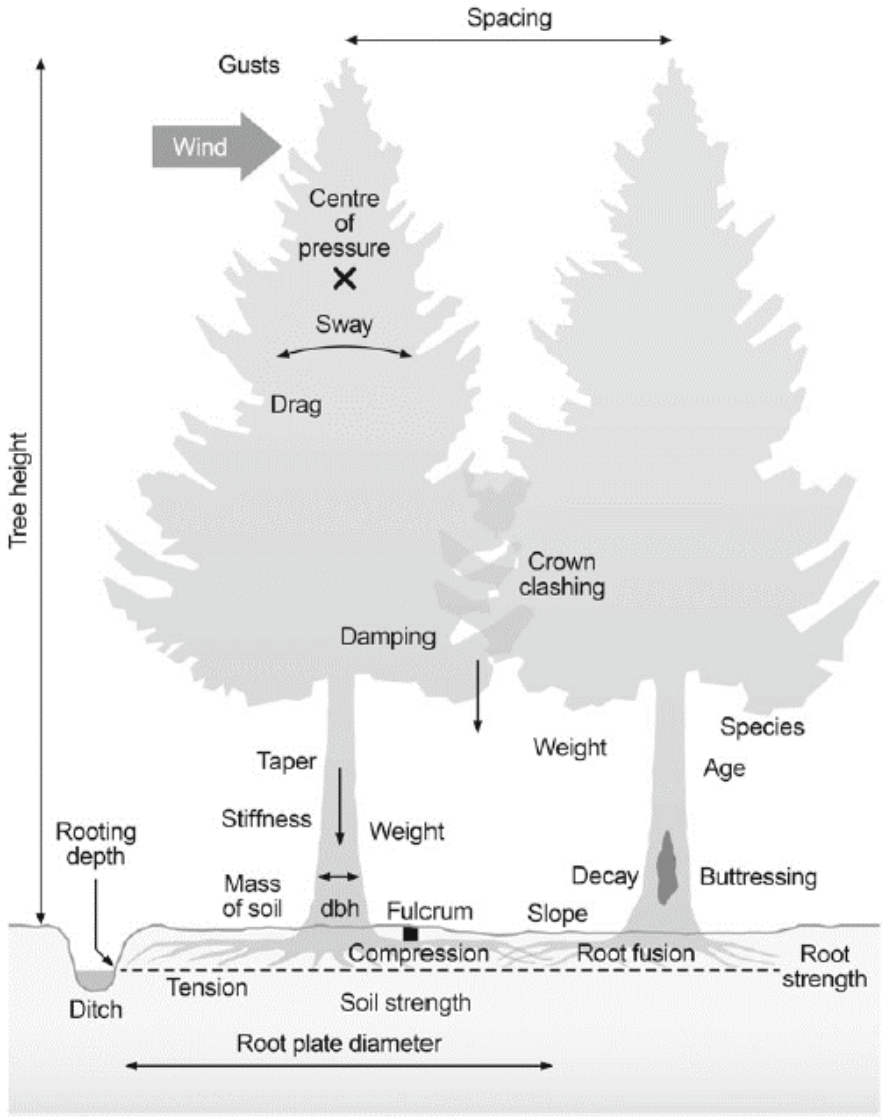

Figure 2-1 Mechanical stability of trees associated to strong winds (Quine, 1995)

2.3 Tree-roots and stability

The below ground portion of a tree is called the rooting system. It performs several important functions such as providing anchoring and support for the tree, absorption and conductance of water and minerals, food storage, and the production of plant growth regulators.

Trees which are shallow rooted form a “plate” shape like rooting system. This root plate can spread over large areas near the surface of the soil. In order for shallow rooted trees with no significant

taproot to achieve anchorage, the roots must transfer forces that the tree experiences into the soil (Stokes et.al, 1996). The two main forces are:

- The gravity loads from the tree
- The bending moments due to eccentricity in gravity loads and lateral wind loads (uplift forces)

Trees are normally subjected to horizontal forces by the action of wind on the canopies (resulting in bending moments that can result in overturning), which are in turn transmitted to the root systems by the stems, causing rotation of the root plates.

Figure 2-2 shows a view of a shallow rooted anchorage system of a tree. The windward lateral roots must be able to transmit rotational torque to the soil by resisting upward forces. The windward fibrous and sinker root systems that are so good at preventing vertical uprooting will help the trees resist rotation. Resistance to rotation requires at least one rigid element at the base of the stem to act as a lever; this can be provided by a taproot, or the lateral root systems, or both (Ennos & Fitter, 1992).

Figure 2-2 Left: Tree failure at Fourth Ave (2014),. Right: Tree failure at Pasir Ris, Singapore (2012); adopted from Rahardjo et al 2016

Trees commonly develop a root plate system (Coutts, 1983) consisting of large diameter lateral roots which radiate almost horizontally from the base of the trunk before tapering and branching (Figure 2-3). These thick, horizontal roots may, in turn develop ‘sinker’ roots which grow vertically downwards. In such systems the resistance of the soil to downwards movement of the roots is high because of their large area and high resistance to compression of the soil.

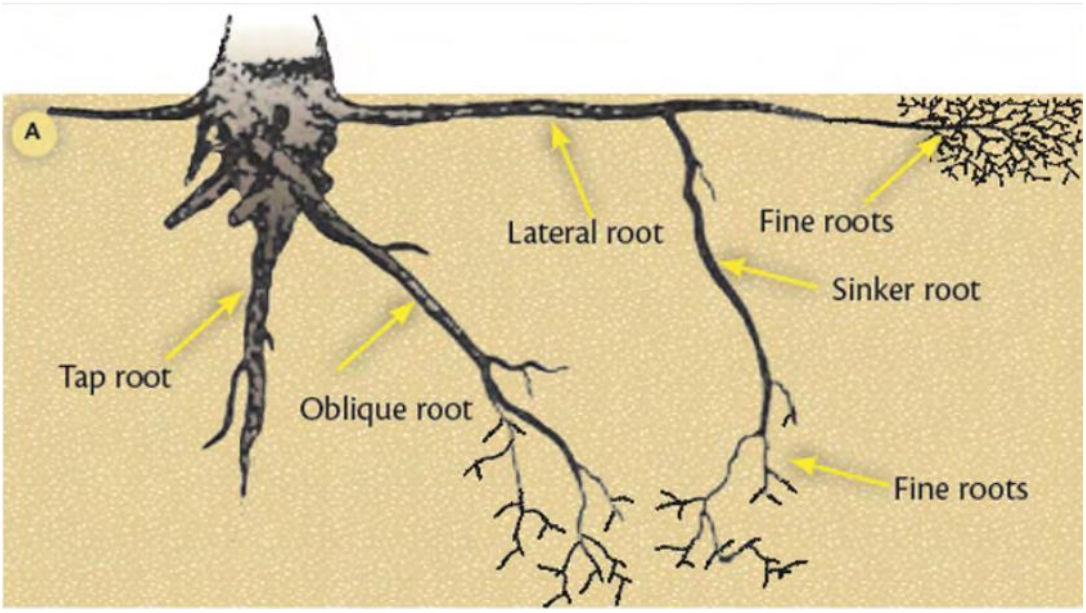

Figure 2-3 Types of roots in the rooting system of common tree species. (Costello et al., 2011)

There are four main components to the anchorage of such systems (Figure 2-4): i) The bearing capacity of the soil; ii) The resistance of the leeward hinge to bending, iii) The resistance of the windward roots, especially the sinkers, to uprooting; and iv) The mass of the root plate-soil plate (Coutts, 1986; Ennos, 2000). The leeward side of the root-soil plate acts as a cantilevered beam, and as a force is applied on the windward side so upward movement of the root-soil plate on that side occurs accompanied by sequential breakage of sinker roots and uplift of the root plate. Eventually the tree overturns with a characteristically elliptical shaped root-soil plate attached; damage to leeside roots occurs nearer to the stem base (Coutts, 1983).

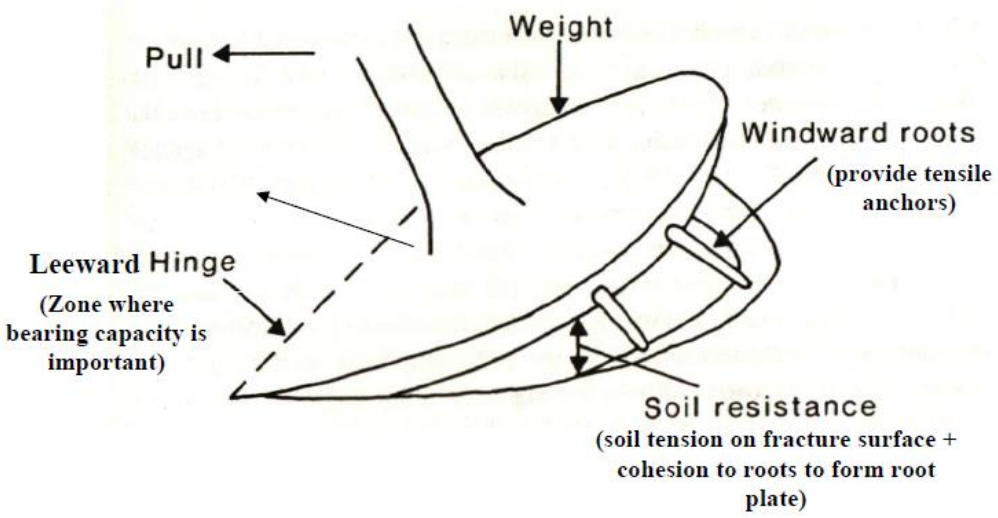

Figure 2-4 Shallow-rooted tree explaining the four components of the anchorage which resist overturning or bending moments (adapted from Coutts, 1983)

Figure 2-5 shows a schematic of a shallow rooted mature tree with sinkers (Danjon et al., 2009). This shows that the compression hinge formed is in agreement with the schematic by Mattheck & Breloer (1994) shown in Figure 2-5 there is another two restraining components highlighted. These are the guying zone and the root plate weight. However, the guying zone has a very small moment arm to the hinge and cannot contribute much restraint. Similarly, the weight of the root plate is only defined by the distance between the compression and tension flexion hinge with the restraining moment arm which is only half of this distance. The biggest contribution to the restraint against toppling is the magnitude of the compression hinge restraint.

There have been many empirical models developed to quantify root plate anchorage. Field observations have led Elie & Ruel (2005) to state that the total root plate anchorage is contributed by the windward roots growing beyond the root plate edge, however, root plate mass and leeward roots did not provide an explanation of the mechanism leading to uprooting. Coutts et al. (1999) stated that tree anchorage resistance factor of safety against wind throw was a function of the product of the tree mass, root plate mass and the root plate radius divided by the product of the wind load and the height to the crown centre of the wind load force.

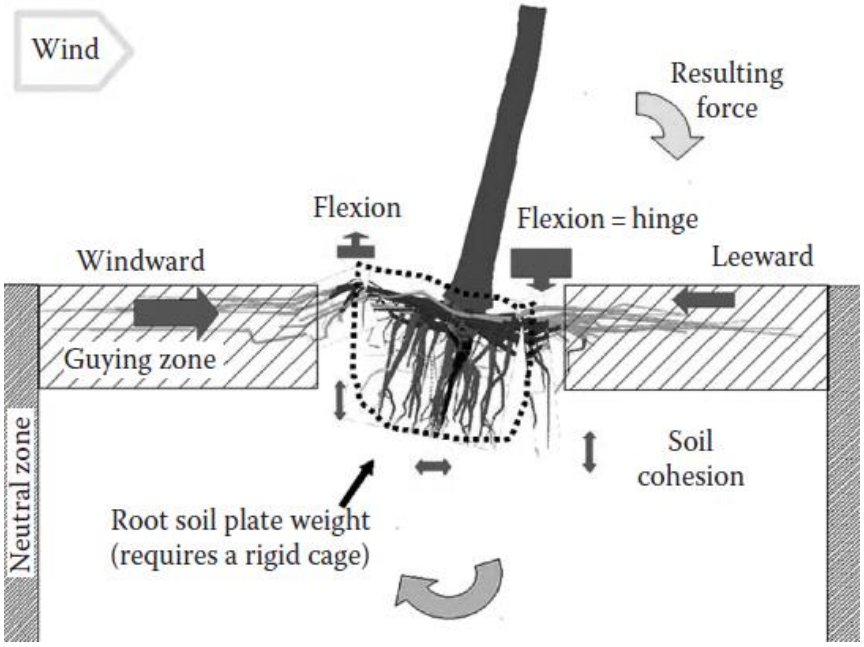

Figure 2-5 Schematic of a mature tree root system with secondary sinkers' when laterally loaded to the right by wind (guying zone has practically no moment arm to the hinge) (Danjon et al., 2009)

The function by Coutts et al. (1999) was based on the conservation of forces but made no mention of greenwood properties, root dimensions, anchorage mechanisms and soil properties. Fourcaud et al. (2008) also stated that tree anchorage was observed to be the product of root plate mass and leeward hinge distance from the stem base. However, the hinge formation due to rupture of the leeward lateral roots and the effects of sinker roots were not accounted for. Anderson et al. (1989) observed that uprooting resistance was a function of the square of the root plate radius divided by the wind load. Lundstrom et al. (2008) provided an equation, stating that the root plate volume

contributing to anchorage was a function of the root plate diameter parallel to the wind direction multiplied by the root plate diameter perpendicular to wind direction multiplied by an empirical factor.

The root plate concept is valuable in understanding and educating practitioners about root anchorage. An accurate model must improve the current models by accounting for greenwood strength, lateral root dimensions and distributions, sinker root dimensions and distributions, failure root plate shapes and soil shear strength.

2.4 Antecedents

This review supports the tree stability analysis base on some case studies that focus specifically on the perceptions of risk as related to the failure of an individual tree. Furthermore, it exemplifies the fact that tree stability is not a local concept and conversely is present worldwide.

2.4.1 Singapore environment

Figure 2-6 shows a failure occurred on Singapore Botanical Garden on the 40 m tall Tembusu tree. According to Straits time news the 270-year-old tembusu tree had already been there when the Gardens was established in 1859, the accident took the life of a 38-year-old woman from India; signs of rot were not visible, said the expert during the review into Botanic Gardens tragedy after tree fell.

Figure 2-6 Singapore Botanical Garden accident caused by tree failure.

2.4.2 Colombian environment

Tree failure cases in Colombia are more common that it appears to be for example the Figure 2-7 to Figure 2-9 present three recent cases in Colombia related to rainfall-induced failure by uprooting. These cases show how important and frequent is the phenomenon. However, the lack of knowledge limits its identification, control and design of remedial measurements.

Figure 2-7 Tree failure on Calazans neighbourhood due to high rainfall intensity on 11th March/2019 leave several damages to infrastructure.

Figure 2-8 Tree collapse accident took the life of a civilian from Cucuta city in Sardinata Roadway on 23rd April/2019

Figure 2-9 Tree uprooting caused several damages to local housing in Cartagena and two habitants got injured during the rainfall of 7th June/2019.

2.5 Structural analysis of trees

The structural properties of trees must be determined in order to evaluate their strength and stability, particularly in relation to their ability to withstand wind loads under storm conditions. In urban areas it is important to assess the risks associated with tree failure so that managers can make decisions on whether to keep or remove a tree.

This section reviews previous studies of trees that have taken a structural perspective and have used engineering methods. The application of engineering structural theory to plant biomechanics has led to a greater understanding of loads on trees and their growth responses to these loads. There have been considerable studies using static methods but there have been only limited studies of the dynamic response in high winds of large open grown trees in the field.

Structural analysis examines the response of a structure to an applied load. It means that depending on the nature of the loading and the response of the structure static or dynamic analysis can be carried out. Biomechanics applies the main principles of structural engineering theory to the study of plant forms, including trees. A fundamental hypothesis is that plants cannot violate the laws of physics (Niklas 1992). In summary, the term "Biomechanics" refers to the study of trees as structural elements, using engineering and physical principles to understand the structural properties of trees and how they interact with the environment.

The first quantitative structural analysis applied to a tree was an attempt to calculate its maximum size. The tree was considered as a tapered pole and only static methods were used. The analysis evaluated the gravitational loads of self-weight of the tree and the maximum height before it failed under its own weight. There was no consideration of branches and there was no attempt to investigate dynamic response of the tree under wind loading. The analysis was applied to a pole made of a homogeneous material which was a simplification used to approximate a tree.

In the last twenty years there has been advances studies of tree structures using static methods. Advances in the technology of instrumentation and data logging has allowed more accurate measurements at high speeds which has resulted in dynamic methods of tree analysis being more widely used. Niklas (1992) summarises the history of trees and describes the basic principles of structural engineering theory which are being applied to the study of plant forms. However, care must be taken in applying well developed engineering beam theory to trees, as green wood differs from normal engineering material.

A mechanical approach to tree biomechanics, using some mathematical simplifications was used by Mattheck and Breloer (1994) to develop the axiom of uniform stress which described a concept whereby growth of the tree is in response to the applied loads. This work highlighted the importance of understanding the loads that a tree endures during its life and explained how the growth response of a tree can influence the stresses that develop within the structural components of the trunk and the branches. The mechanical analysis was limited to a static approach where loads were considered to be constant. This is valid for gravitational forces of weight, snow and ice, especially on large trees in forests where dynamic forces such as wind may not be significant. The static approach does not represent the conditions where rapidly changing loads occur, especially loads due to wind. Mattheck

and Breloer (1998) considered wind as a statically applied force, and any variations were considered by changing the value of the static load.

2.5.1 Slope-deflection equations

The slope-deflection relates the rotation of an element (both rotation at the ends and rigid body rotation) to the total moments at either end. The aim is to compute the end moments for each member in the structure as a function of all the degrees of freedom (DOFs) associated with both ends of the member. From there, the equilibrium conditions at all the joints can be solved for the unknown rotations.

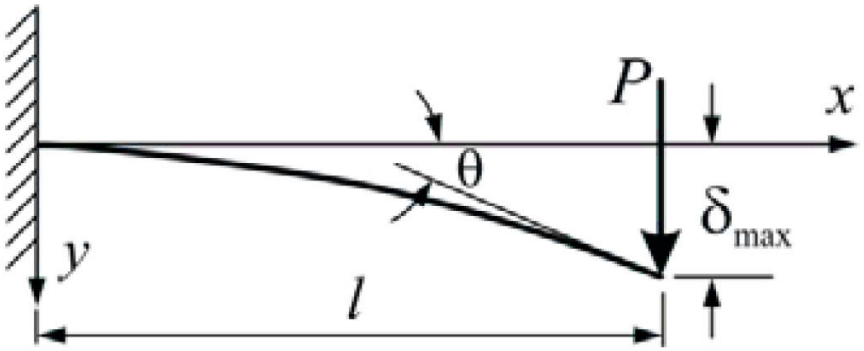

Figure 2-10 Slope-Deflection Equation for cantilever beam

This is the system of equations that we will have to solve, where the equations are the equilibrium equations for each node and the unknowns are the translations and rotations of the nodes.

$$\delta_{max} = \frac{P.l^3}{3EI} \qquad \text{(Eq. 1)}$$

where,

δ_{max} : Maximum displacement of the beam element under the applied load

P : Applied load

l : Beam length

E: Elastic Young modulus

I : Second moment of inertia

2.6 Static tree pulling test

When describing the loading regime in beams when they are subjected to pure bending, engineering textbooks often emphasise on the longitudinal stresses that are set up. When a beam of uniform cross-section is bent, the concave surface is subjected to longitudinal compression and the convex surface is subjected to longitudinal tension, the stress increasing linearly away from the neutral axis which is located at the centroid of the cross-section.

The resistance of each element to bending is proportional to the square of its distance from the neutral axis; this is because it is both stretched more when further away from the neutral axis, and because its moment arm about the neutral axis is greater. The flexural rigidity *R* of a beam is therefore given by the expression.

$$\sigma = \frac{M_y}{I} \qquad \text{(Eq. 2)}$$

where M_y and I (eq. 2) are the bending moment and second moment of inertia respectively.

$$I = \frac{\pi d^4}{64} \times T_R \qquad \text{(Eq. 3)}$$

The longitudinal stress σ_L in a part of the beam positioned a distance *y* from the neutral axis, when a bending moment *M* is applied is given by the expression.

$$\sigma_L = \frac{My}{I} \qquad \text{(Eq. 4)}$$

The maximum stress, $\sigma_{L_{max}}$, occurs at the inner and outer edges of the beam and is given by the expression.

$$\sigma_{L_{max}} = \frac{My_{max}}{I} \qquad \text{(Eq. 5)}$$

where y_{max} is the greatest distance from the neutral axis.

According to Ennos (2009), In engineering materials such as metals, ceramics and plastics, which are stiff and isotropic and have low breaking strains, this analysis is perfectly adequate. Beams made of brittle metals and ceramics will fail on the tension side and then simply break right across, while those composed of ductile metals will instead bend irreversibly when the yield stress of the metal is reached, conserving their cross-section.

2.7 Resisting moments of trees under static loading

The resisting moments of the tree have been measured for Sitka spruce (Picea sitchensis) (Coutts, 1983) and found to depend on the resistance of the hinge at the base of the trunk, the soil tension, the soil shear, the strength of the windward roots, and the weight of the root-soil plate.

The combined resisting moment as a function of angle of inclination to the vertical is shown Figure 2-11and the curve was considered typical of many found in tree pulling experiments (England et al., 2000).

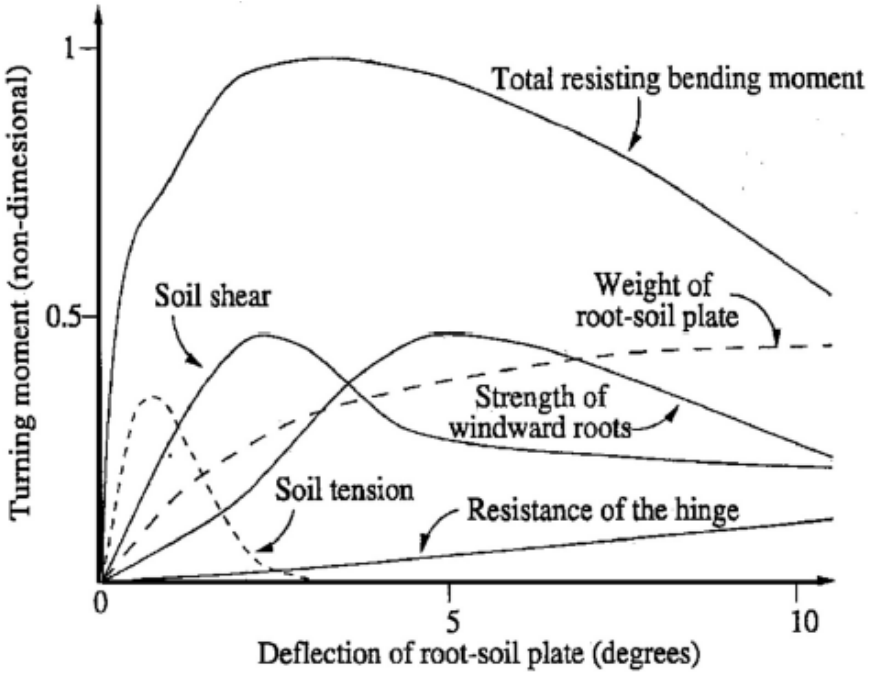

Figure 2-11 Combined resisting moment as a function of leaning angle from a typical tree pulling test experiments. (England et al, 2000)

In tree failure prediction, there was an attempt to correlate critical turning moment to tree size and particularly to stem weight or volume. The best predictive variable used the expression (H x DBH2); (H was height and DBH was trunk diameter at breast height) which was also used by Moore (2000). This variable was used as the x axis in Figure 2-12 but could not completely explain the variability in the critical turning moment. The slenderness ratio of the forest trees ranged from 54 to 82.

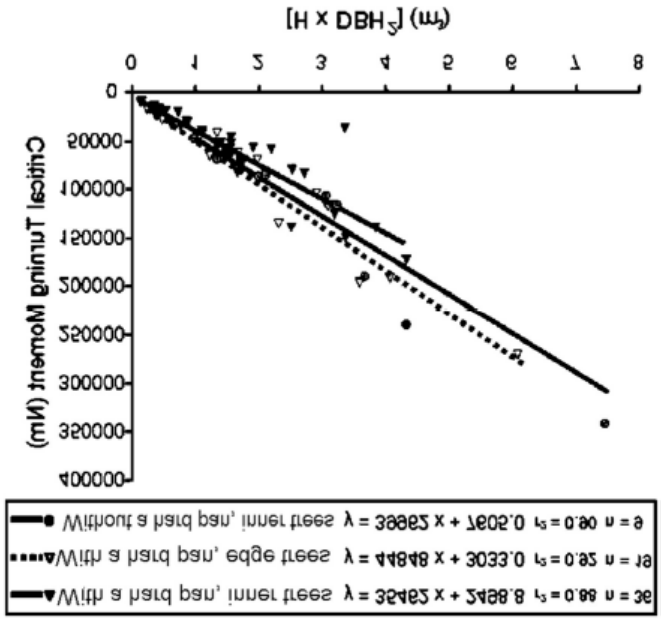

Figure 2-12 Static tree pull results. Maximum overturning moment is 350 kN.m. all related to equation ($H.DBH^2$) to predict stability and failure (from Cucchi et al., 2004)

The results from these tests found that the static pull test over-estimated the bending moments needed to cause failure and estimated critical wind speeds greatly exceeded real wind speeds recorded during a gale which caused tree damage.

Tree pulling tests in Finland on Scots pine, Norway spruce and birches in frozen and unfrozen soil were conducted by Peltola et al. (2000) to evaluate mechanical stability. The maximum resistive bending moment before failure was most significantly and positively correlated with diameter at breast height (DBH) and tree height (H). The best predictor of BM_{max} for uprooting was the relationship H x DBH^2, and the best predictor of BM_{max} for stem breaking was the relationship H x DBH^3.

Tree pull tests were conducted on 164 radiata pine tree (Pinus radiata) in New Zealand on six different soil types (Moore, 2000). Trees were pulled with a hand winch and maximum resistive bending moments were recorded when the trees failed. Three failure modes were observed, stem failure, root failure and uprooting with a maximum bending moment value of 300 kN m being recorded (Figure 2-13). Trees with a high taper (low slenderness ratio) had higher maximum resistive bending moment than trees with low taper. There was a positive correlation for bending moment with tree height, diameter at breast height and stem volume. Using the relationships between DBH and H to predict the uprooting/wind throw failures did not describe the mechanisms of uprooting.

Assessing the risk of failure of trees has been hampered by a lack of empirical data with respect to assessment of structural defects. Therefore, tree pulling tests have been used in research to determine the resistance of trees against rupture and up-rooting. Many tests have been conducted by applying

a load with a winch to pull forest trees until they uprooted, or the stem failed (Papesch et al., 1997; Moore, 2000; Peltola et al., 2000).

These tests are designed to cause ultimate failure and therefore lead to the destruction of the subjected trees. Such studies have explored tree failure mechanisms to predict the critical turning or bending moment to cause failure. In addition, a non-destructive assessment of tree risk was required to identify hazardous trees and to be able to retain mature trees. However, tree pulling tests focused only on assessing the likelihood of failure. There was no study carried out on the estimation of overall stiffness of trees using the tree pulling tests for numerical implementation purpose.

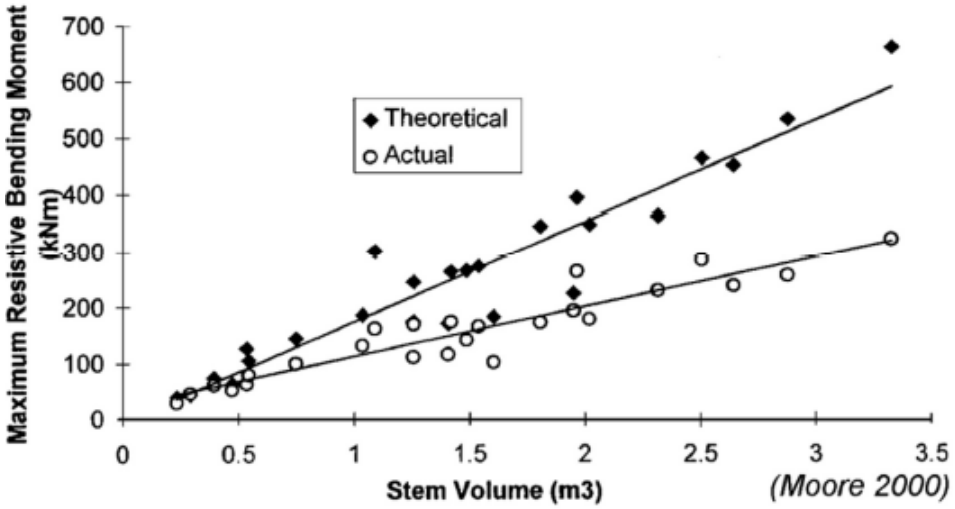

Figure 2-13 Stem failure was seen in 29 out of 164 Pinus radiata in NZ. The maximum stem failure resistive bending moments (kN.m) were compared to the theorical values calculated (from Moore, 2000).

2.8 Numerical Simulations

The first case studies on tree uprooting mechanisms and the development of the first systematic method of analysing tree anchorage were based on the experimental work done by Coutts (1986). The method involved the assessment of the impacts of different anchorage elements on Sitka spruce tree species, i.e. root-soil weight, root material strength under tension and soil strength on the overturning resistance of spruce.

This method led to the first mechanistic model of tree anchorage that described the root anchorage strength and performance in terms of the resisting elements on the tree. Understanding of the anchorage mechanism progressed with the use of numerical analysis and advances in plant architecture (Dupuy et al., 2005b, 2007; Fourcaud et al., 2008). This approach used the finite element method (FEM) to calculate the deformation of root-soil systems in three dimensions. simulated root systems with their specific architectural properties were considered in the simulations. These analyses allowed a comparison of the theoretical anchorage performances of different root types. In

addition, Fourcaud et al. (2008) attempted to quantify the relative roles of root components, in anchorage strength in different soil types using a simple 2-D FEM model.

2.8.1 Saturated soil media

In an unsaturated soil, the flow of water is a problem of clear significance to geotechnical engineers and soil scientists. This fact is substantiated by the abundance of literature that has appeared on the subject (Fredlund 1979; Justo and Saertersdal 1979; Schreiner 1986; Alonso et al. 1987; Fredlund and Rahardjo 1993). The brief explanations provided below aim only to provide a context for the particular theoretical approach used here - no attempt is made at providing a full review of the subject at this point.

Traditionally, for a saturated soil, there are two main types of stability analysis considered which are total stress analysis and effective stress analysis (Lambe and Whitman 1969). Total stress analysis is generally used to analyse a recently cut or constructed slope (i.e. short-term period) and it is assumed that the water pressure in the slope has had no time to dissipate. The strength parameters of that analysis are defined using Mohr-Coulomb failure envelope in terms of total stresses and porewater pressures are not required. On the other hand, effective stress analysis is normally applied for a long-term slope stability analysis. The strength parameters are described by Mohr-Coulomb failure envelope and the effective shear strength concept provided by Terzaghi. However, such analyses focus on saturated conditions and therefore, by definition, do not need to include any contribution to shear strength from negative pore water pressures (suctions).

Rahardjo et al. (2009) developed a finite element model of root anchorage and used a parametric study to examine the influence of soil properties. Thus, numerical models have been used essentially to investigate the influence of root architecture on tree anchorage using theoretical parameters for soil and roots. Less is known about the failure mechanism, which is crucial for predicting the occurrence of uprooting. This implies to better understand the effect of soil–root friction, root strength and soil strength on the whole response of the root system involved in the overturning process.

2.9 References

- Costello LR, Hagen BW, Jones KS (2011) Oaks in the urban landscape: Selection, care, and preservation. Oakland, CA: University of California Agriculture and Natural Resources Publication 3518.
- Dupuy L, Fourcaud T, Stokes A. (2005). A numerical investigation into factors affecting the anchorage of roots in tension. European Journal of Soil Sciences. 56:319-327.
- Fourcaud, T., Ji, J.N., Zhang, Z.Q., Stokes, A., (2008). Understanding the impact of root morphology on overturning mechanisms: a modelling approach. Ann. Bot. 101, P1267–1280.

- Rahardjo, H., Leong, E. C., Qin, Q. S., Fong, Y. K., Lee, D. T. T., Wee, J. D., Harnas, F. R., Min, R. and Amalia, N. (2016). "Effect of rainfall on tree stability". NTU-NParks Collaborative Research Report, Nanyang Technological University, Singapore, 315 p.
- Rahardjo, H, N. Amalia, E.C. Leong, F.R. Harnas, T.T. Lee, and Y.K. Fong (2017) "Flux Boundary Measurement to Study Tree Stability", Landscape and Ecological Engineering, Vol.13, Issue 1, January 2017, pp.81-92.
- Blight, G. E. (1997) The "Active Zone in Unsaturated Soil Mechanics. 1st GRC Lecture, Nanyang Technological University, Singapore.
- Wood, C.J. (1995). Understanding wind forces on trees. In Coutts, M.P., and J. Grace (Eds.). Wind and Trees. Cambridge University Press, Cambridge, U.K. pp. 133–163.
- Peltola, H.M., (2006). Mechanical stability of trees under static loads. Am. J. Bot. 93, 1501–1511.
- Gardiner BA, Byrne K, Hale SE, Kamimura K,Mitchell SJ, Peltola H, Ruel J-C (2008) A review of mechanistic modelling of wind damage risk to forests. Forestry 81(3):447–463. https://doi.org/ 10.1093/forestry/cpn022
- Peltola H, Gardiner B, Nicoll B (2013) Mechanics of wind damage. In: Gardiner B, Schuck A, Schelhaas M-J, Orazio C, Blennow K, Nicoll B (eds) Living with storm damage to forests: what science can tell us. Eur Forest Inst, Joensuu, pp 31–38
- Niklas, K.J. (1992). Plant Biomechanics. An engineering approach to plant form and function. University of Chicago Press. Uni. Chicago.
- Mattheck & Breloer (1994) Field guide for visual tree assessment (VTA), Arboricultural Journal, 18:1, 1-23, DOI: 10.1080/03071375.1994.9746995
- Mattheck C & Breloer H (1998) The body language of trees: A handbook for failure analysis; TSO.
- Stokes, A., and C. Mattheck. (1996). Variation of wood strength in tree roots. Journal of Experimental Botany 47:693–639.Ennos & Fitter, 1992
- Coutts MP (1983) Root architecture and tree stability. Plant Soil 71:171–188
- Coutts, M. (1986). Components of tree stability in Sitka spruce on peaty grey soil. Forestry 59:173–197.
- Ennos AR (2000) The aerodynamics and hydrodynamics of plants. J Exp Biol 202:3281–3284
- Danjon F, Fourcaud T, BertD (2005) Root architecture and wind-firmness of mature Pinus pinaster. New Phytol 168(2):387–400. https://doi.org/10.1111/j.1469-8137.2005.01497.x
- Elie J-G , Ruel J-C (2005) . Windthrow hazard modelling in boreal forests of black spruce and Jack Pine, Can. J. For. Res., vol. 35 (pg. 2655 -2663)

- Coutts MP, Nielsen CCN, Nicoll BC. (1999). The development of symmetry, rigidity and anchorage in the structural root system of conifers. Plant and Soil 217: 1–15.
- Lundström, T.; Jonsson, M.J.; Kalberer, M. (2007a) The root-soil system of Norway spruce subjected to turning moment: Resistance as a function of rotation. Plant Soil, 300, 35–49.
- Lundström, T.; Jonas, T.; Stöckli, V.; Ammann, W. (2007b) Anchorage of mature conifers: Resistive turning moment, root-soil plate geometry and root growth orientation. Tree Physiol., 27, 1217–1227.
- England, A.H., C.J. Baker, and S. Saunderson. (2000). A dynamic analysis of windthrow of trees. Forestry 73:225–237.
- Moore, J.R. (2000). Differences in maximum resistive bending moments of Pinus radiata trees grown on a range of soil types. Forest Ecology and Management 135:63–71.
- Peltola, H., S. Kellomaki, A. Hassinen, and M. Granader. (2000). Mechanical stability of Scots pine, Norway spruce, and birch: An analysis of tree-pulling experiments in Finland. Forest Ecology and Management 135:143–153.
- Papesch, A.J.G., J.R. Moore, and A.E. Hawke. (1997). Mechanical stability of Pinus radiata trees at Eyrewell Forest investigated using static tests. New Zealand Journal of Forestry Science 27:188–204.
- Quine CP, Gardiner BA, Coutts MP, Pyatt DG (1995) Forests and wind: management to minimise damage. For Comm Bull 114. HMSO, London
- Blackwell P G, Rennolls K and Coutts M P (1990) A root anchorage model for shallowly rooted Sitka spruce. Forestry 63,73–91.
- Fredlund, D. G. (1979) "Appropriate concepts and technology for unsaturated soils." Can. Geotech. J., 16, 121 - 139.
- Justo, J. L. and Saertersdal R. (1979) "Design parameters for special soil conditions." General Report, Proc. 7th Eor. Conf. SMFE 4, 181 - 208.
- Schreiner, H. D. (1986) "State of the art review of expansive soils for TRRL." Imperial College, London,
- Alonso, E. E., Gens, A. and Hight, D. W. (1987) "Special problem soils." Ninth European Conf. on Soil Mechanics and Foundation Engineering: 1087-1146.
- Fredlund, D. G. and Rahardjo, H., (1993) "Soil Mechanics of Unsaturated Soils." John Wiley & Sons: New York,
- Lambe, T.W. and Whitman, R.V. (1969) Soil Mechanics. John Wiley & Sons, New York.
- Rahardjo H, Harnas FR, Leong EC, et al. (2009) Tree stability in an improved soil to withstand wind loading. Urban for Urban Green 8:237–247

- Coutts MP (1983) Root architecture and tree stability. Plant Soil 71:171–188
- Coutts, M. P. (1986). Components of Tree Stability in Sitka Spruce on Peaty Gley Soil. Forestry, 59(2), 173A–197.
- Dupuy L, Fourcaud T, Stokes A. (2005). A numerical investigation into factors affecting the anchorage of roots in tension. European Journal of Soil Sciences. 56:319-327.
- Fourcaud, T., Ji, J.N., Zhang, Z.Q., Stokes, A., (2008). Understanding the impact of root morphology on overturning mechanisms: a modelling approach. Ann. Bot. 101, P1267–1280.

3. RESEARCH PROGRAM-METHODOLOGY

3.1 Introduction

Assessing the risk of failure of tress has been hampered by a lack of empirical data with respect to assessment of structural defects. Therefore, tree pulling tests have been used in research to determine the resistance of trees against rupture and up-rooting. Many tests have been conducted by applying a load with a winch to pull forest trees until they uprooted, or the stem failed (Papesch et al., 1997; Moore, 2000; Peltola et al., 2000).

These tests are designed to cause ultimate failure or preloading and therefore lead to the destruction of the subjected trees. Such studies have explored tree failure mechanisms to predict the critical turning or bending moment to cause failure. In addition, a non-destructive assessment of tree risk is required to identify hazardous trees and to be able to retain mature trees. However, tree pulling tests focused only on assessing the likelihood of failure. There was no study carried out on the estimation of overall stiffness of tress using the tree pulling tests for numerical implementation purpose. Figure 3-1 presents the flowchart conducted for each stage in order to a reliable and statistical analysis for each tree-rooting species.

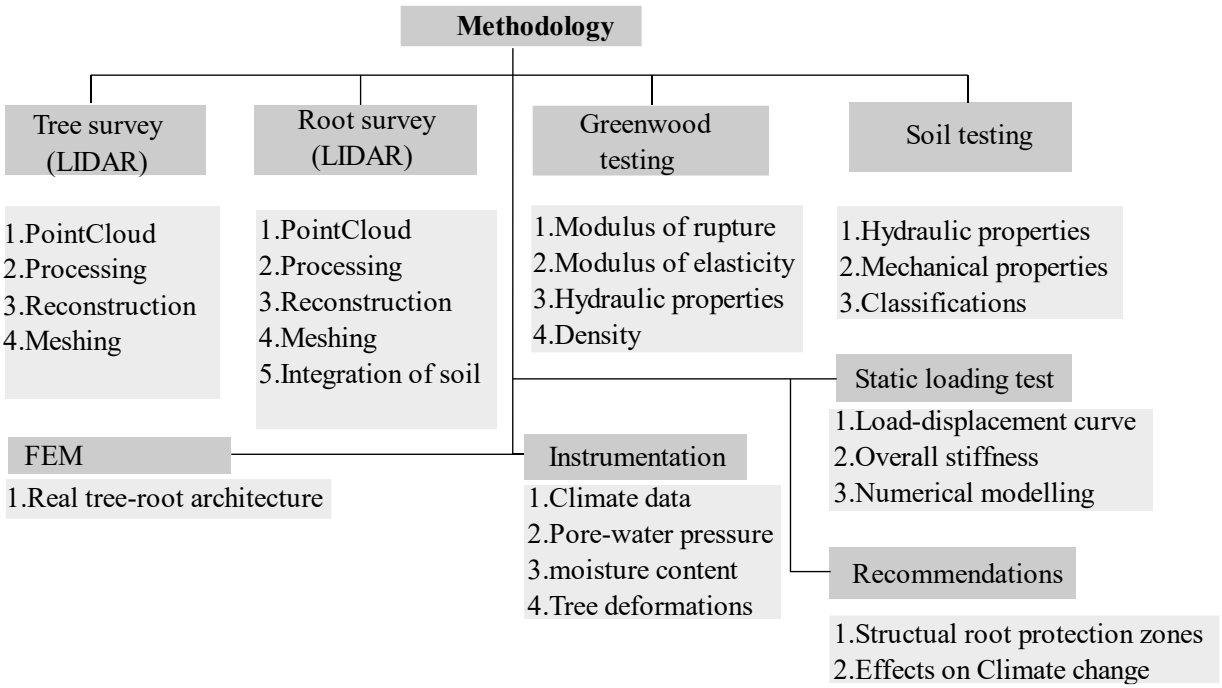

Figure 3-1 Outline research program

3.2 Site and tree selection

A study area was established where the tree species of *S. saman*, *K. senegalensis* and *S. grande* trees were planted. These trees were tested and instrumented to study the overall biomechanical response and the plant-water relationships of the trees. The study site was located within the Changi Village state land (1.389286°N, 103.985810°E), in the Eastern part of Singapore Island. The climate in the study region is characterized by a tropical climate with constantly high temperatures, and a considerable amount of rainfall during the year. Based on National Environmental Agency of Singapore, the mean annual rainfall in the last 35 years in the specific zone was around 2250 mm (Figure 3-2) and the mean annual temperature was around 27.7°C (Chow & Roth,2006: MSS,2017).

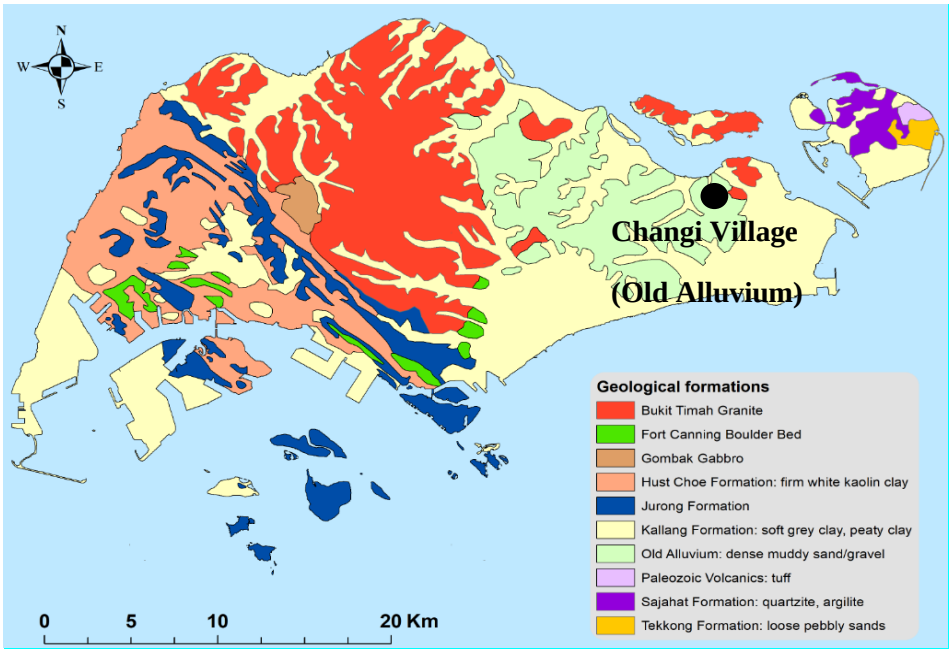

Figure 3-2 Study area within the geological map of Singapore (Adapted from DSTA, 2009)

Figure 3-3 shows the tree species selected around the study area, the main advantages of the selection are the statistical representativity of this species around all Singapore, and the availability to extent the results obtained on this research to a global panorama of the Country.

Figure 3-3 Selected trees at Changi Village, (a) *Syzygium grande*, (b) *Khaya senegalensis*, (c) *Samanea Saman*

The field Instrumentation installed was designed to acquire climatic, ground water table, soil hydraulic properties, and tree movement data during the monitoring period.

The climatic data included different weather conditions (rainfall, solar radiation, relative humidity, air temperature, wind speed, wind direction). The changes in soil parameters such as pore-water pressures and volumetric water contents due to changes in the climate were recorded. In addition, the tree movement and the ground water table variation due to changes in local climatic conditions were recorded.

3.3 Soil sampling and testing

Laboratory classification tests consisting of sieve analysis (ASTM C136), Atterberg limits (ASTM D4318), natural moisture content (ASTM D2216) and organic content (ASTM F1647) were performed on selected soil samples. The test results indicate that the predominant soil is clean sand (SW) with a unit dry weight of 12 ± 0.2 kN/m^3 and an organic content ranging between 3 to 7%. The observed organic content was related to the topsoil layer or near surface soils that had been previously modified with time through cut and fill operations for the construction of former settlements. Consequently, almost all the first 10 cm soil in the project area could be considered as some variety of modified urban topsoil.

Table 3-1 Soil index properties at Changi Villagr

Site Soil Properties		**Changi Village**
Depth		0 - 4.0m
USCS Classification		SW - Clean sand
Percentage of gravel, sand, fines		0%, 95%, 5%
Saturated permeability	k_s	3.0×10^{-5} m/s
Unit weight	ρ_d	12 kN/m^3
Specific Gravity	G_s	2.6
Liquid Limit	LL	NA
Plasticity Index	PI	NA

3.3.1 Tree survey characteristics

The geometrical characteristics of the tree samples tested are presented in Figure 3-1, describing tree diameter, average stand age and the loading procedure to be applied in the field. The IN and NIN sub symbols refer to the installation of additional instrumentation during the static loading test.

Table 3-2 Geometrical characteristics tree species tested.

Tree	ID	Height (m)	Tree diameter (m)	Stand age (year)	**F**ailed/**L**oaded
K. senegalensis (Senegal mahogany)	IN-01	7.6	0.7	≈ 25	L
	IN-02	7.6	0.7		L
	NIN-01	9.3	0.5		L
	NIN-02	9.3	0.5		F
S. saman (Rain tree)	IN-01	6.5	0.7	≈ 25	L
	IN-02	6.5	0.7		L
	NIN-01	9.8	0.5		L
	NIN-02	9.8	0.5		F
S. grande (Sea apple)	IN-01	6.4	0.7	≈ 25	L
	IN-02	6.4	0.7		L
	NIN-01	11.2	0.8		L
	NIN-02	11.2	0.8		F

The mechanical properties of the wood for each species were obtained from previous studies presented by Lee, 2016 and the additional values obtained from the 3-point bending tests carried out on tree branch and root samples collected after the tree loading tests and air spading. The specific mechanical properties are presented in Table 3-3.

Table 3-3 Mechanical properties tree species

Tree Species	Unit weight (kN/m^3)	MOE (GPa)	ν	MOR σ_{ymax} (GPa)
K. senegalensis	8.0	0.8	0.3	40.1
S. saman	8.0	2.0	0.3	31.6
S. grande	8.0	1.0	0.3	50.2

***** MOE= Modulus of Elasticity, ν = Poisson's ratio, MOR = Moduli of Rupture reported by **Lee (2006)**

3.4 Static loading test

The static loading tests were performed using a rope attached to the trees at different locations along the trunk to apply controlled static lateral loads to the trees. These lateral loads were measured using a load cell in line with the pulling rope.

The static loading tests were performed by winching a rope in steps of 0.05 m until a cumulative rope deformation of 0.6 m was reached. During the tests, the trees were not loaded beyond the elastic limit. This was to ensure that the tests did not damage the trunk, causing permanent deformation or

uprooting the tree. Figure 3-4 a) shows the pictorial setup for the static loading tests. There was a pulley advantage of two (2) times for this test.

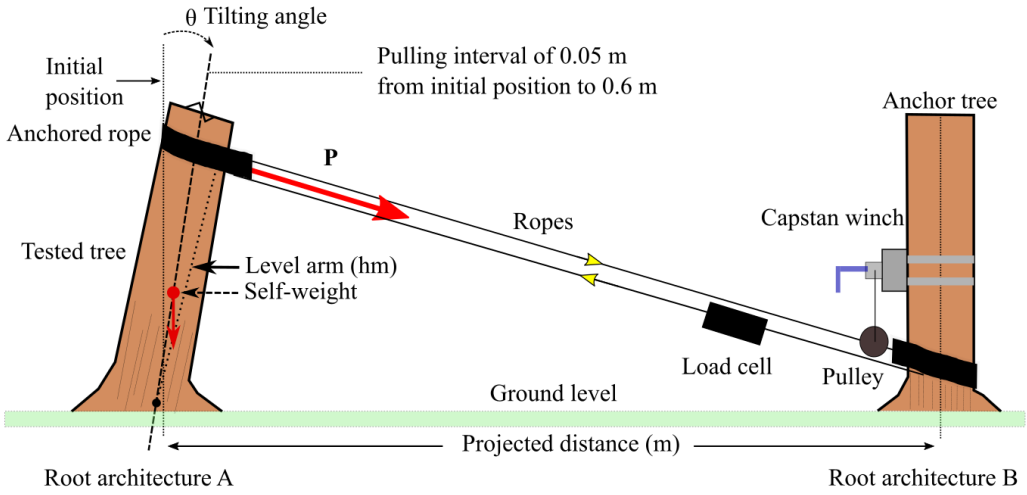

(a)

(b)

Figure 3-4 Static pull test a) Setup for the static loading test b) capstan winch and winching point of test tree

The applied lateral loads, deformations and geometry of the tree were recorded and used to compute the strength parameters, strains and stresses developed within the trunk in order to estimate the overall stiffness of the tree anchored to the ground. The main assumption was to consider the tree as a tapered cantilever column with a restrained end where the soil restrains the lateral deformation and the entire load that is applied to the soil through the trunk and the root architecture.

Table 3-4 Steps involved in the bending mechanics analysis (Modified from Ludstrom, 2007a)

Step	Description
1	Calculation of σ due to the applied force (DIN 52 186). The maximum σ, independent of type of failure, corresponds to ε_{max}.
2	Calculation of the elasticity in bending (*E*) due to applied force (DIN 52 186), corrected for the shear deformation by using slope-deflection equations.
3	Definition of MOE as the gradient of the straight line between $\sigma(\varepsilon_E) = 0$ and $\sigma(\varepsilon_E) = \sigma_{max}$. The initial deformations associated to the rope are not included in the ε_E data.
4	Calculation of Δ: Δ is the tilt angle from no load until the end of the test.

3.5 Air spading

Air spading is a pneumatic method to use compressed air to perform excavations without applying too much pressure onto the tree bark. The soil within the rooting zone was clean sand and suitable for the air spading method. Air spading was found to be an excellent method for revealing the rooting architecture and extents of the tree roots in this study.

Figure 3-5 (a) exposed root plate of the air spaded *S. grande.* (b): Lifted exposed root plate of the air spaded *K. senegalensis* in preparation for laser scanning.

Figure 3-5 shows that the soil was a sandy soil and even within the same soil, different species of trees developed different rooting architectures. The *S. grande* developed a flat root while the *K. senegalensis* developed a heart root.

3.6 Laser scanning of tree-root system

For each of the tree species that was air spaded, the actual root architecture was very different in terms of type, depths and orientations. These root architectures were captured through laser scanning using the V-Line 3D Terrestrial Scanner RIEGL VZ-400 (3D TLS capable of providing data with

an accuracy of 5 mm). VZ-400. The VZ-400 is a compact and lightweight surveying instrument, mounting in any orientation and even under limited space conditions. RIEGL VZ-400 provides high speed, non-contact data acquisition using a narrow infrared laser beam upon RIEGL's unique echo digitization and online waveform processing, which allows achieving superior measurement capability even under adverse atmospheric conditions and the evaluation of multiple target echoes. The line scanning mechanism is based upon a fast-rotating multi-facet polygonal mirror, which provides fully linear, unidirectional and parallel scan lines.

Figure 3-6 REIGL VZ-400 terrestrial scanner with the attached top mounted NIKON full frame camera used in this investigation

3.7 Numerical modelling and verification

A FE mesh for the tree-root-soil system and the applied boundary conditions. The mesh extended a distance of 3 times beyond the edges of the rooting architecture and a depth of 3 times beneath the rooting depth, which was found to be sufficient to prevent boundary effects. At the sides of the mesh, no lateral movement was permitted, and full fixity was imposed at the base of the mesh.

- The meshing tool software MESHLAB and 3D-modelling software SPACECLAIM were used to generate suitable meshes and 3D solids as input for the finite element modelling of the three (3) species of trees, which are rain tree (*S. saman*), African mahogany (*K. senegalensis*), and sea apple (*S. grande*)
- Finite element modelling software MIDAS GTS-NX was used for numerical analysis of two (2) species of trees, which were rain tree (*S. saman*) and African mahogany (*K. senegalensis*).

- During the field tests, the depth of the ground water level was below the tree roots, and thus the soil within the rooting zone was considered as unsaturated soil.

3.7.1 Simulation set-up

Simulations were performed to replicate the field experiment as presented in Figure 3-7. The stem height at which the pulling force was applied was 2.5 m. The soil domain (10 m x 10 m x 6 m) was meshed with hybrid 8-node elements, with the region containing the roots meshed into finer elements with an approximate edge size of 0.05 m. Symmetrical boundary conditions were imposed on the four laterals of the soil domain so that these faces were blocked to constrain soil motions.

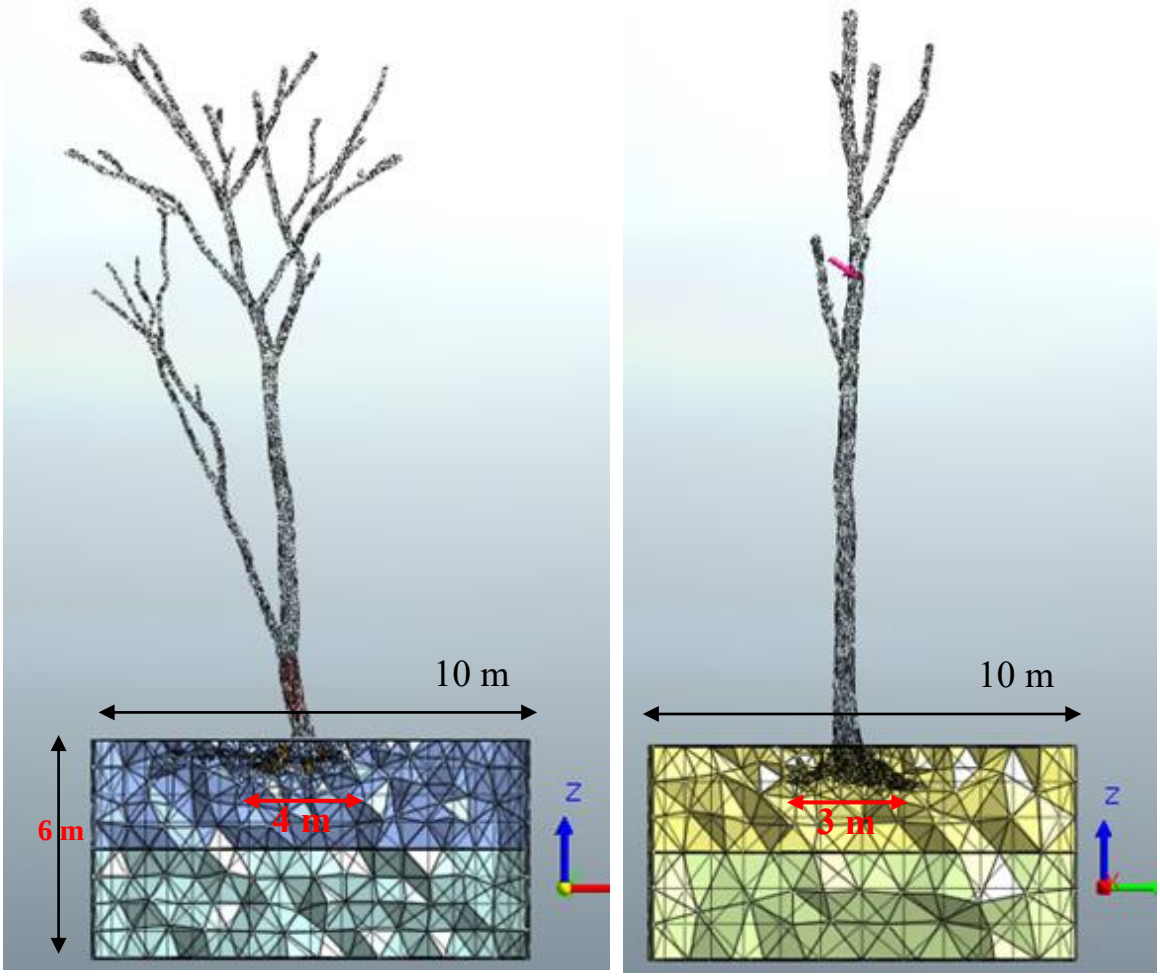

Figure 3-7 Numerical model domain and border conditions.

Static loading was applied on the soil-root system in two steps: the gravity body force was applied first with the gravity constant g = 9.81 m/s^2, then a horizontal displacement was imposed in the direction of the x axis at the top of the stem to ensure a maximum deflection angle regarding to the loading steps; this displacement implies large deformations in the root-soil system which makes sure that maximum turning moment occurs largely before the end of the simulation. The reaction force and corresponding displacement at the top of the stem were recorded during the simulation.

This approach uses the finite element method (FEM) to calculate the deformation of root–soil systems in three dimensions. Real root systems with their specific architectural properties were considered in the simulations; these simulations allowed comparison of the theoretical anchorage performances of different root types. In addition, the study attempted to quantify the relative roles of root components, e.g. superficial laterals, deep roots and tap roots, in anchorage strength in different soil compaction conditions using different Young modulus.

In this new model, the developments were focused on root–soil interaction, the mechanical behaviour of root material and the characteristics of the soil. Due to the complexity of meshing root architecture with 3-D solid elements, the roots were considered as embedded beam elements for *S. saman* and *K. Senegalensis* trees (See Figure 3-8 and Figure 3-9. We evaluated the relevance of this choice in a preliminary study carried out a realistic comparison based on the stiffness of the soil, purpose of the research and state of art in this kind of simulations. Simulations considering roots modelled with embedded beam elements were compared with field test and root–soil interface properties.

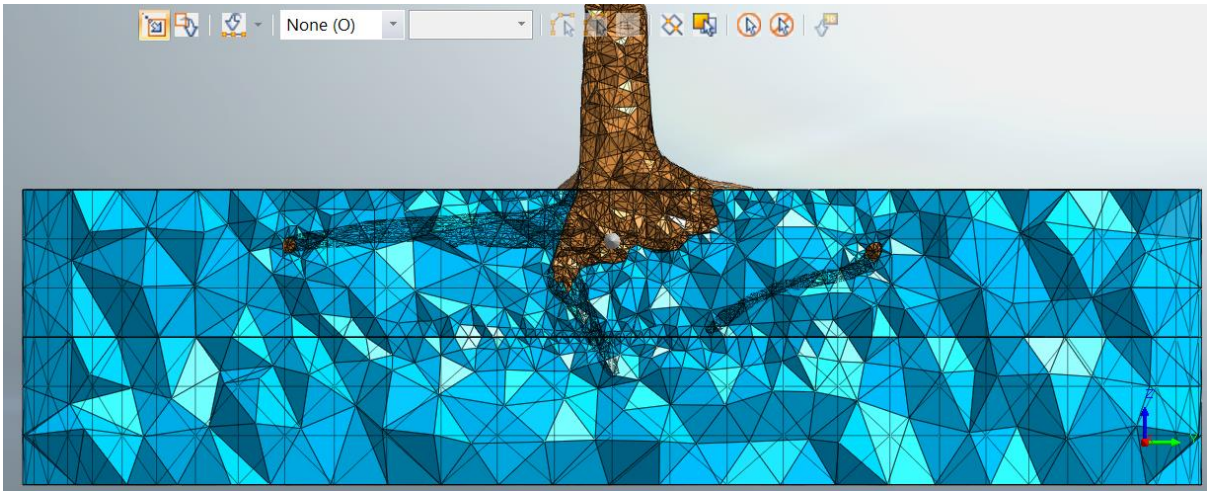

Figure 3-8 Bonded contact interface in *S. Saman* tree.

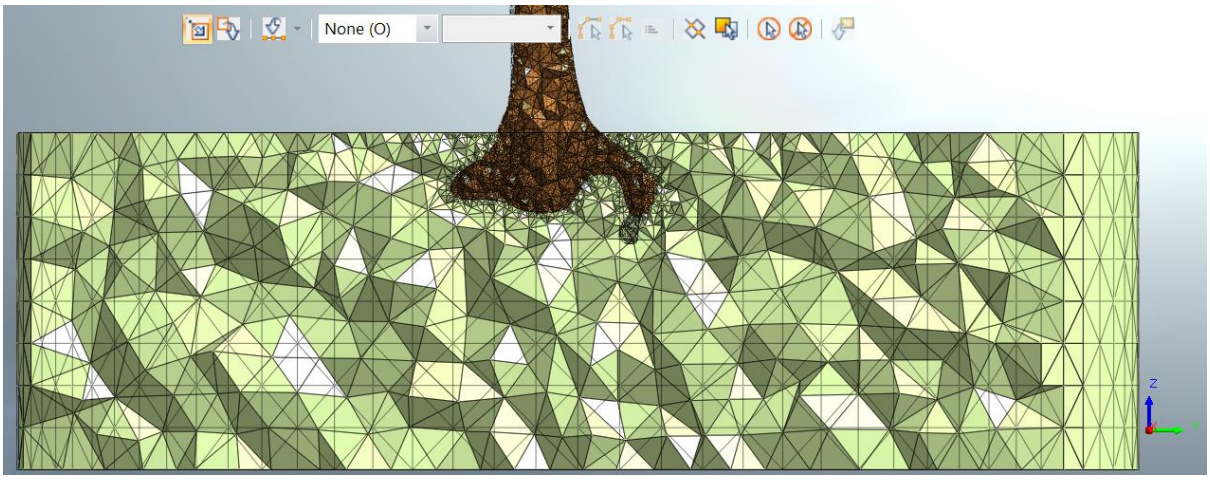

Figure 3-9 Bonded contact interface in *K. Senegalensis* tree.

Embedded beam elements were then used in the anchorage model, implying that all the roots were slender structures embedded in the soil region. The roots were meshed with 8-node linear Timoshenko beam elements with hybrid cross sections. The anchorage model described above allows the tree anchorage behaviour of various tree species to be modelled under different soil conditions. In our study, we found a specific case of two (2) tree species planted in sandy soil. The inputs of the model were:

- Scanned rooting system excavated after an in-situ tree-pulling experiment.
- Soil properties obtained in laboratory.
- Root material properties from data taken from the literature and tree pulling test.

The model outputs were expressed by using response curves, i.e. “turning moment” versus “deflection angle at the stem base”.

3.8 References

- Chow WTL, Roth M (2006) Temporal dynamics of the urban heat island of Singapore. International Journal of Climatology 26, 2243–60.
- MSS 2017. Annual climate assessment (2017) Singapore report. Technical report, Meteorological Service Singapore.
- Defence Science and Technology Agency (DSTA) (2009): Geology of Singapore (2nd Edition), DSTA, Singapore.
- ASTM D4318-00, Standard Test Methods for Liquid Limit, Plastic Limit, and Plasticity Index of Soils, ASTM International, West Conshohocken, PA, 2000.

- ASTM C136 C136M-14, Standard Test Method for Sieve Analysis of Fine and Coarse Aggregates, ASTM International, West Conshohocken, PA, 2014.
- ASTM D2216-10, Standard Test Methods for Laboratory Determination of Water (Moisture) Content of Soil and Rock by Mass, ASTM International, West Conshohocken, PA, 2010.
- ASTM F1647-11, Standard Test Methods for Organic Matter Content of Athletic Field Rootzone Mixes, ASTM International, West Conshohocken, PA, 2011.
- Lee, D. T. -T. (2016). Effect of rainfall on tree stability. Doctoral thesis, Nanyang Technological University, Singapore.
- Lundström, T.; Jonsson, M.J.; Kalberer, M. The root-soil system of Norway spruce subjected to turning moment: Resistance as a function of rotation. Plant Soil 2007a, 300, 35–49.
- Lundström, T.; Jonas, T.; Stöckli, V.; Ammann, W. Anchorage of mature conifers: Resistive turning moment, root-soil plate geometry and root growth orientation. Tree Physiol. 2007b, 27, 1217–1227.
- P. Cignoni, M. Callieri, M. Corsini, M. Dellepiane, F. Ganovelli, G. Ranzuglia, (2008) MeshLab: An Open-Source Mesh Processing Tool, Sixth Eurographics Italian Chapter Conference, page 129-136.
- MIDAS GTS NX, “Verification &Application Manual”, 2014

4. RESULTS

4.1 Tree-root geometry and root architecture

For each of the tree species that was air spaded, the actual root architecture was very different in terms of type, depths and orientations. These root architectures were captured through laser scanning using the V-Line 3D Terrestrial Scanner RIEGL VZ-400 (3D TLS capable of providing data with an accuracy of 5 mm). The laser scanning was conducted after the static loading test on the excavated tree-root systems. The collected point cloud was post-processed to obtain the final configuration of the root architecture. It is important to mention that due to the difficulties in the reconstruction of the root architecture the third-order roots and below were removed.

- ***K. senegalensis***

The *K. senegalensis* root system consisted of a central trunk of an average diameter of 0.8 m with a two-sided first order root with an average root diameter (d_r) ranging between 0.1 to 0.15 m; the depth of the rooting system was about 1.4 m (see Figure 4). The main thicker root structure members had numerous secondary lateral roots. The total volume of the roots was close to 0.81 m^3 and there were three structural roots with a length of 3.0 m in relation to the centre axis of the trunk.

(a) ***(b)***

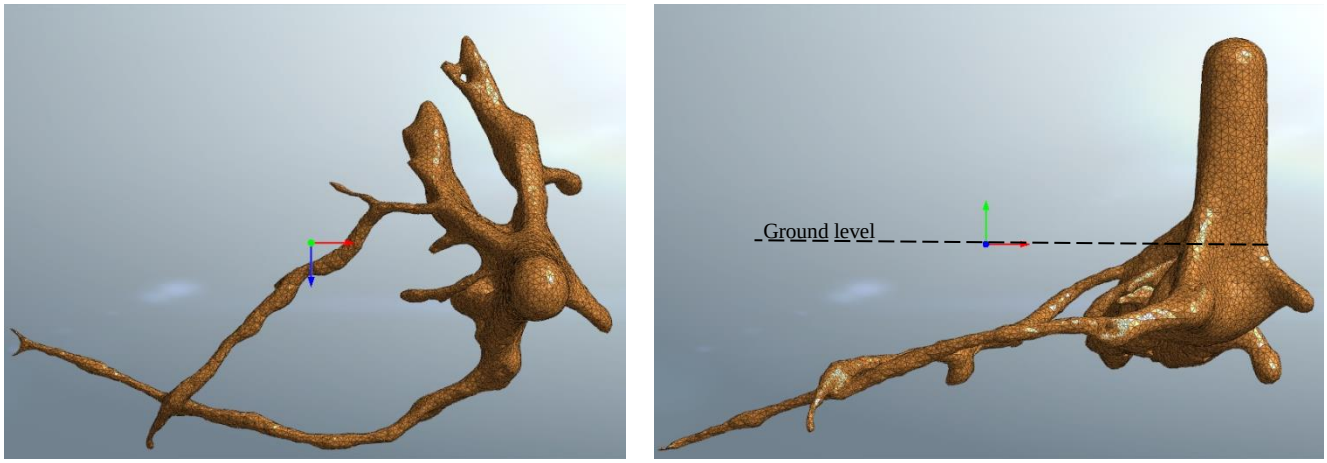

Figure 4-1 Root architecture K. senegalensis (a) Plan view, (b) front view.

- ***S. saman***

The root system of *S. saman* had more structural roots that provided the stability of the tree with an average diameter of 0.5 m for the main trunk and 0.2 m of average root diameter (d_r) for the first order root. Four massive roots radiating horizontally from the trunk were identified. The depth of the rooting system was about 1.2 m (see Figure 5). The main thicker root member had numerous secondary lateral roots. The total volume of the roots was close to 1.1 m^3 and there were four structural roots with a length of 4.2 m measured from the trunk.

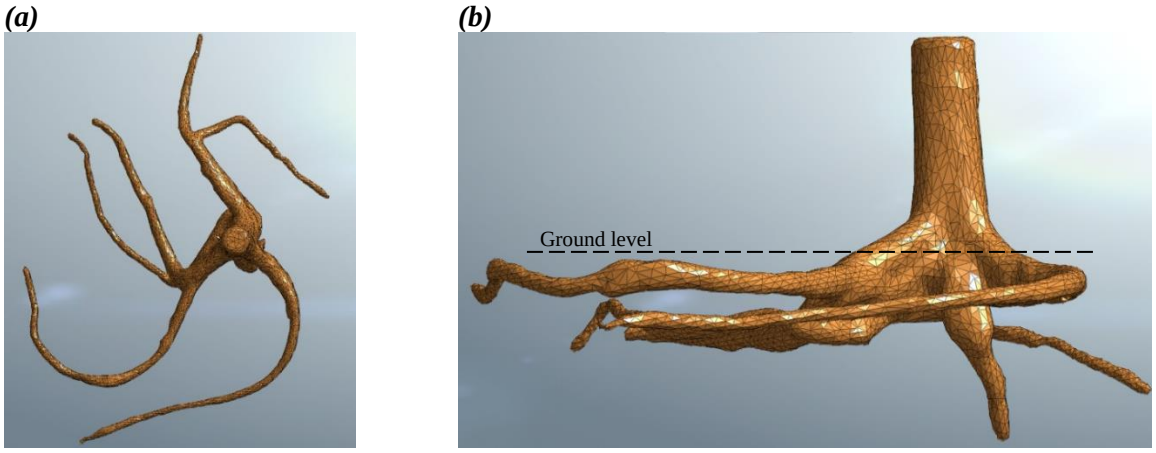

Figure 4-2 Root architecture *S. saman* (a) Plan view, (b) front view.

- ***S. grande***

The *S. grande* root system had a main central structural root system covered by a considerable quantity of secondary shallow roots, each with an approximate diameter of 0.8 m (see Figure 6). The total root volume system was close to 0.8 m^3 and the dominant structure involve four structural roots with a length of 4.2 m. The rooting system was distributed horizontally and could be considered as a root-plate foundation.

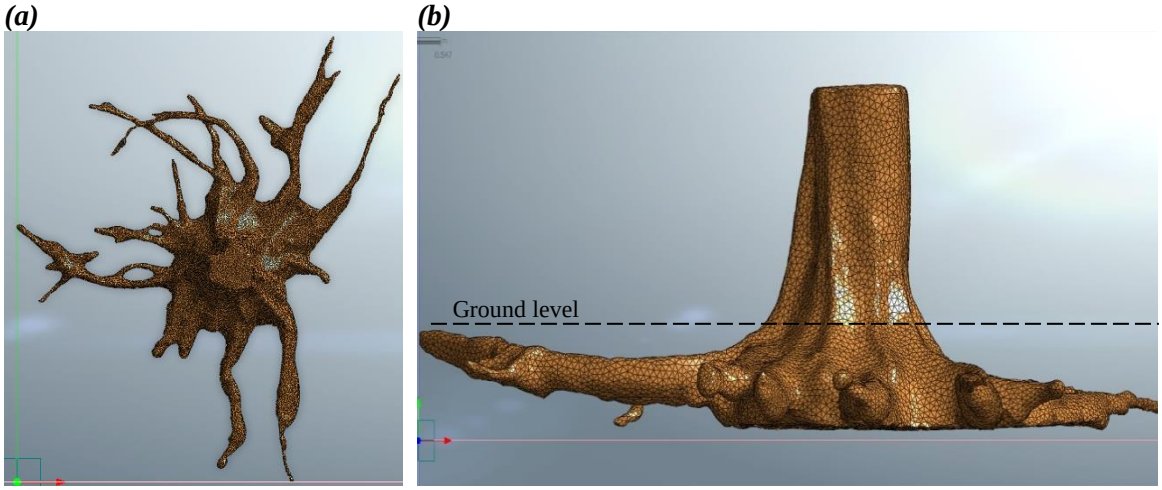

Figure 4-3 Root architecture *S. grande* (a) Plan view, (b) front view.

4.2 Static loading test

Four similar loading tests for each species were performed on trees planted within the same soil type. The loading tests were conducted following the procedures that were consistent with the previous studies (Yang et al., 2017, Cannon et al., 2015, Fourcaud et al., 2008, Lundström 2007a, Nicoll et al., 2006). The tests considered the overall behaviour of trees under a constant displacement around 0.5 m at the top without triggering the uprooting of the tree. The soil within the rooting zones of the trees was classified as clean sand and the groundwater level ranges from 5.0 to 6.0 m at this location. For a general understanding, the "overall stiffness (OE)" is defined as a fully coupled response of the root architecture, soil type and trunk stiffness.

Is well known, that the static load test provides a quantitative approach for non-destructive assessment of the uprooting resistance and is a good indicator of overall stiffness of intact or compromised trunk-root systems. During the tests, the overall load-deformation behaviour was recorded because it has been identified to indicate the anchorage strength of the root.

4.2.1 Sensitivity of individual trees under lateral force

Figure 4-4 presents all the measured data collected from each static loading test, showing that that the load deformation response for each species varies considerably. This variability contributes to the uncertainty about the results derived from the static load tests. The post-analyses of the tests provide the understanding that the tree-root anchorage strength of the tree is not unique, and the rooting architecture plays an important role on the mechanical response of the tree.

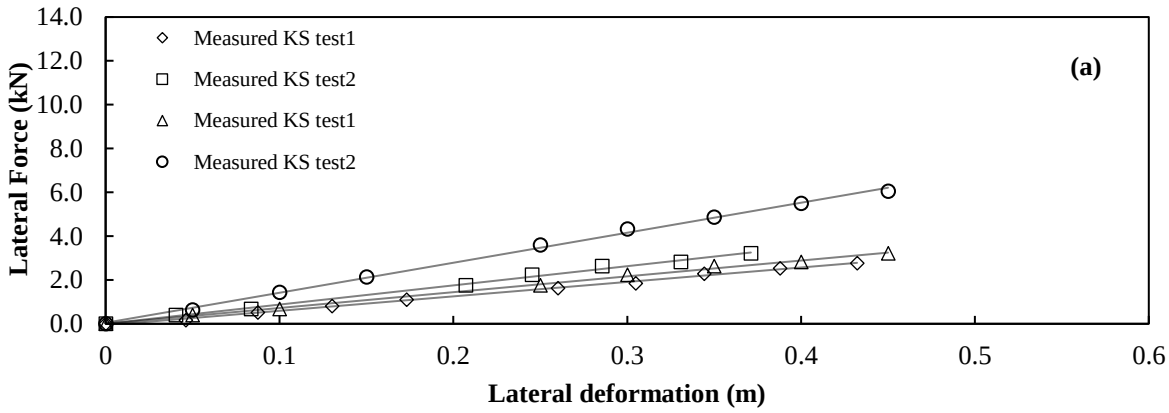

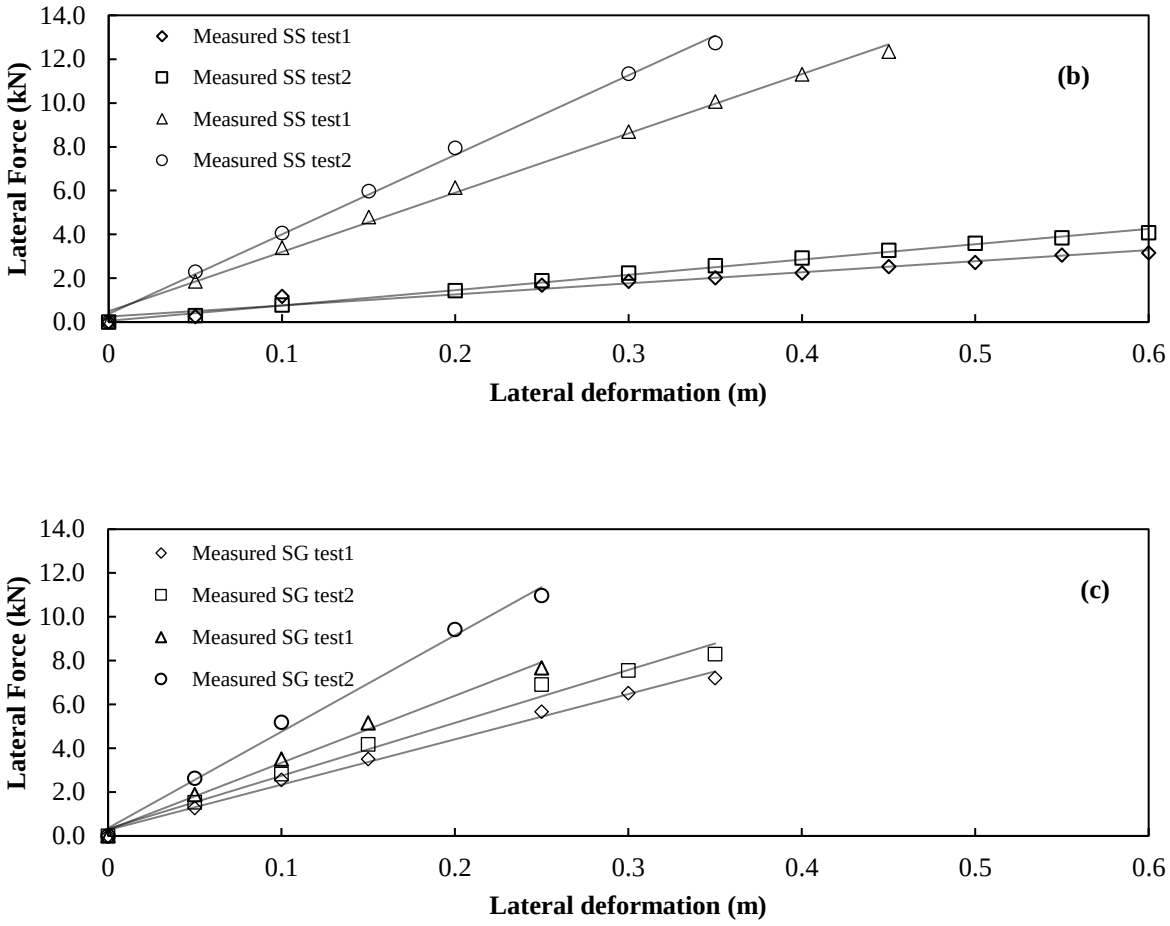

Figure 4-4 Lateral force versus lateral deflection response, a) *K. senegalensis* (KS), b) *S. saman* (SS), c) *S. grande* (SG)

The measured lateral load deformations show a slight non-linearity in the measurements during the application of load increments. This non-linearity is possibly caused by slightly movements of the reaction slings used to secure the equipment. The mechanical response of the individual trees to the static loading tests shows that the load-deformation behaviour is heavily dependent on tree rooting architecture, soil type and soil moisture content within the rooting zone at the time of the test.

- ***K. senegalensis***

The results obtained from the static loading tests on *K. senegalensis* trees showed a slight difference in the overall stiffness that varied between 0.8 and 1.0 GPa. The difference can be due to the different deformations of the rope and slings used, and the different points of application of the load during the initial stage of the loading or trunk imperfections.

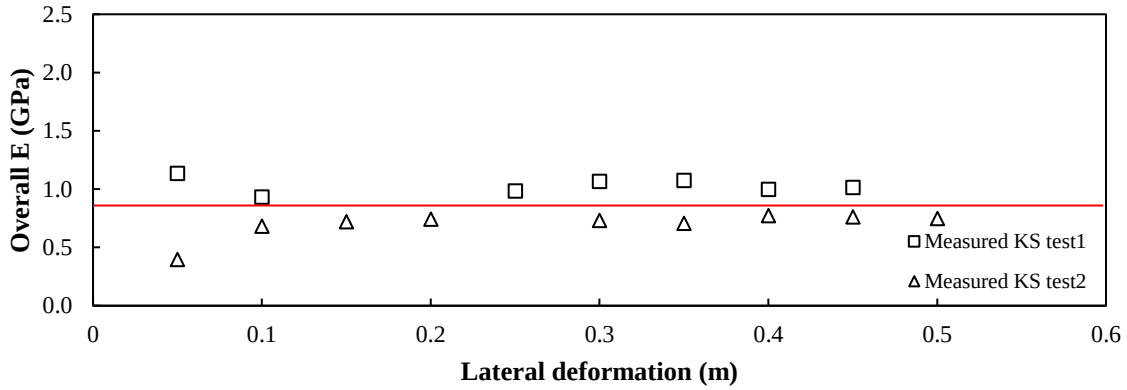

Figure 4-5 Static Loading Test results a) K. senegalensis (KS).

The developed stresses are plotted against lateral deformation produced by the static load in Figure 8. As pointed out by Lavers, (1983), for tropical trees there should be some differences that can be expected between individual trees even within the same group of trees, soil conditions and climatic conditions. This is because the stability of the tree remains strongly influenced by diameter of the trunk, rooting architecture and soil conditions, of which the first two parameters can differ dramatically between trees.

- ***S. saman***

The results obtained from the static loading tests on the *S. saman* trees also showed differences in the results that varied from 1.6 to 2.0 GPa. There was also a good agreement found between the stresses measured from the static load tests and the stresses developed in the numerical analysis that incorporates the OE and those results from the field branch and root's 3-point bending tests.

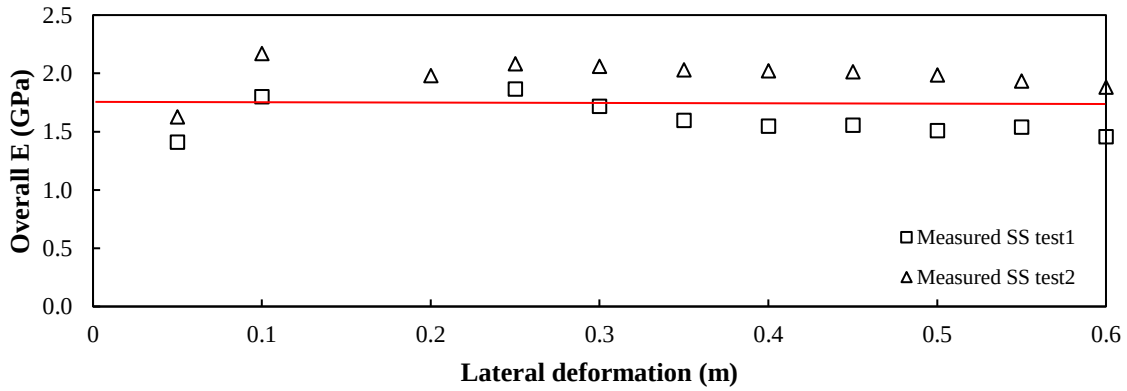

Figure 4-6 Static Loading Test results *S. saman* (SS).

- ***S. grande***

The results obtained from the static loading tests on *S. grande* tree showed a slight difference in the results that varied from 0.81 to 1.23 GPa. The measured data during the static loading tests suggested that the root architecture behaved as a root-plate due to the uniform radial distribution of the root system comprised many small diameter lateral roots.

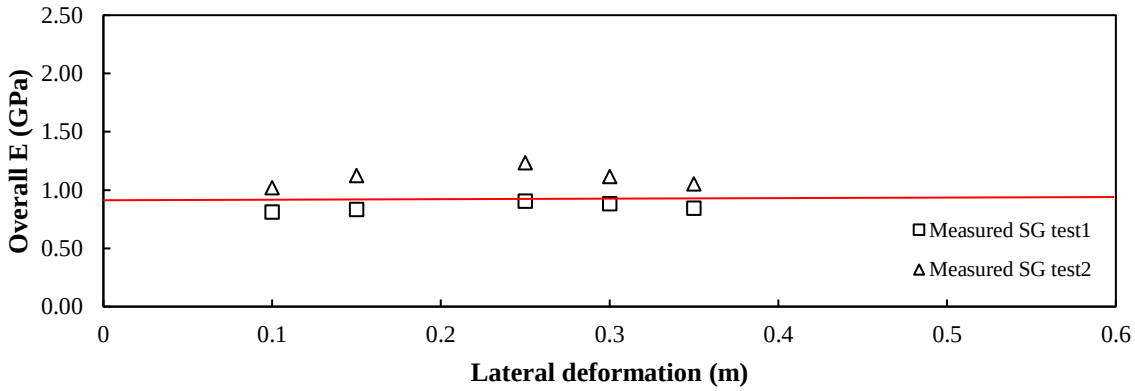

Figure 4-7 Static Loading Test results *S. grande* (SG).

4.3 Numerical modelling

For the numerical modelling, loads on the trees were simulated by applying a horizontal displacement (0.1 m) at 2.5 m above the ground surface. The advantage of considering a fixed displacement instead of lateral load was to avoid inconsistencies due to the static load not being applied at the same point as in the field tests and to normalize the lateral deflection displacement recorded at a higher part of the tree to the point of application in the numerical model. According to Yang et al, (2017) the mechanical response on individual trees needs to be compared to the unique geometry and normalized results of each tree to evaluate the true behaviour of the tree system.

The trunk-root system behaviour obeys the elastic theory, considering a plastic the V-Mises yield surface. Deformation prior to yielding was assumed to be linear elastic governed by the elastic modulus of the trunk E_t = 0.8-2.0 GPa and Poisson's ratio $\nu = 0.3$. The yield stress σ_{ymax} were defined for the tree species by Lee, (2016) and presented in Table 2. Soil was modelled as a elastic perfectly plastic material using the Mohr-Coulomb theory.

Due to the number of secondary roots and the final geometry obtained, the complexity and meshing of the final geometry could not be possible. Therefore, the numerical modelling analysis the *S. grande* tree is not presented due to the numerical errors caused by the condensed point caused by the secondary roots.

The physical connections between the soil-root system has been defined as a bonded condition that describes the link between the surfaces. The following stage consisted of creating the physical links between the soil and roots. Different techniques exist to model explicit surface to surface interaction using constraints implemented with rigid link interface elements. In this case, we use an interface rigid link to allow the interaction between the soil-root system The hypothesis of a bonded root–soil interaction was supported and confirmed by field observations where most of the tree roots remained embedded in the mass of soil after loading, suggesting that most of the soil moved during the static loading process was bonded in the network of roots. Similar findings were reported by Dupuy et al. (2007).

4.3.1 Parametric analysis

A parametric analysis was also conducted to evaluate the influence of elastic modulus of the soil on the overall stiffness of the tree-root-soil system.

As presented in the methodology section, the soil samples collected at the Changi site were tested in the laboratory and corresponded to a well-graded sand (SW) and was considered to behave as homogeneous, elastoplastic material classified using the Mohr-Coulomb strength criteria in the model with a unit weight (γ) of 12 kN/m^3, cohesion (c') of 5.0 kPa and friction angle (φ') of 33° with an elastic modulus ranging from 2.5 MPa for loose sand to 25 MPa in dried compaction condition, . To understand the effect of material properties on the model response, one of the parameters, the elastic modulus of the soil was varied in the parametric analysis from 2.5 MPa to 25 MPa.

It is important to note that the values and directions of the applied displacements in the numerical model corresponded to those applied in the field static loading tests presented earlier. The results obtained in the simulations are summarized for *K. senegalensis* and *S. saman* trees in Figure 4-8, Figure 4-9 and Table 3. The numerical model showed that there was a strong influence of the soil elastic modulus on the overall stiffness of the trees. Using the reference case as E_s = 2.5 MPa, changes in the soil modulus caused changes in the stresses and consequently, the overall stiffness of about up to 30% for the case of *S. saman*.

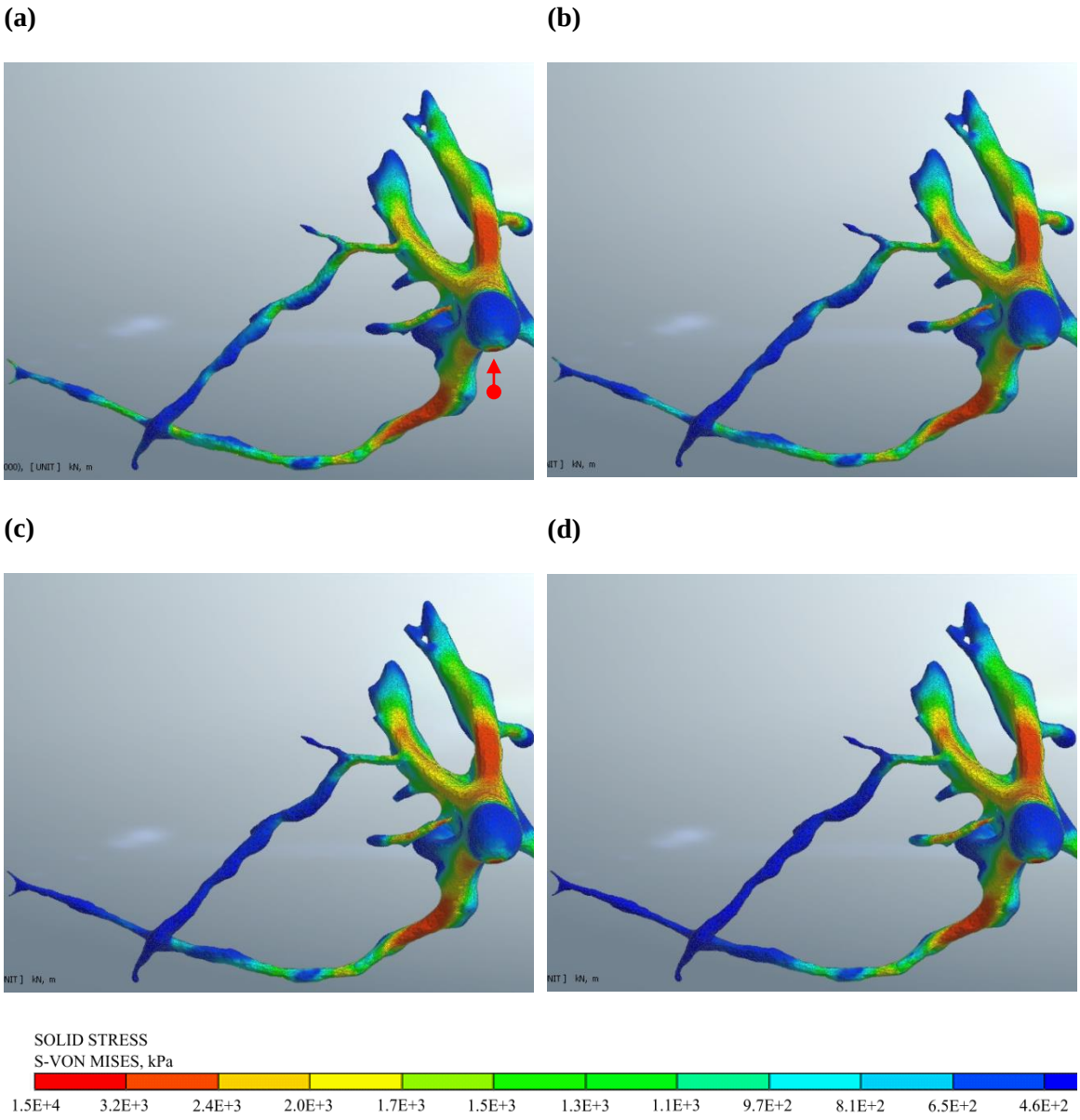

Figure 4-8 Overall stresses of the K. senegalensis tree varying elastic modulus of the soil [(a)-Es= 2.5 MPa, (b)- Es= 5.0 MPa, (c)- Es= 10.0 MPa, (d)- Es= 25.0 MPa].

For *K. senegalensis*, the numerical model predicted a dominant contribution of the first order roots on the overall anchorage strength. The simulation presented on Figure 4-8was also able to display the stress distribution within the model roots under the lateral load. Since wind-induced lateral loads can be simulated using lateral displacements, the results obtained in this numerical modelling can be used to represent the effects of wind on tree stability. In terms of the soil-root interaction, it was found that for the same applied displacement, an increase in the soil elastic modulus caused the stress concentration to increase in the main roots near the trunk and particularly in the windward or tension zone.

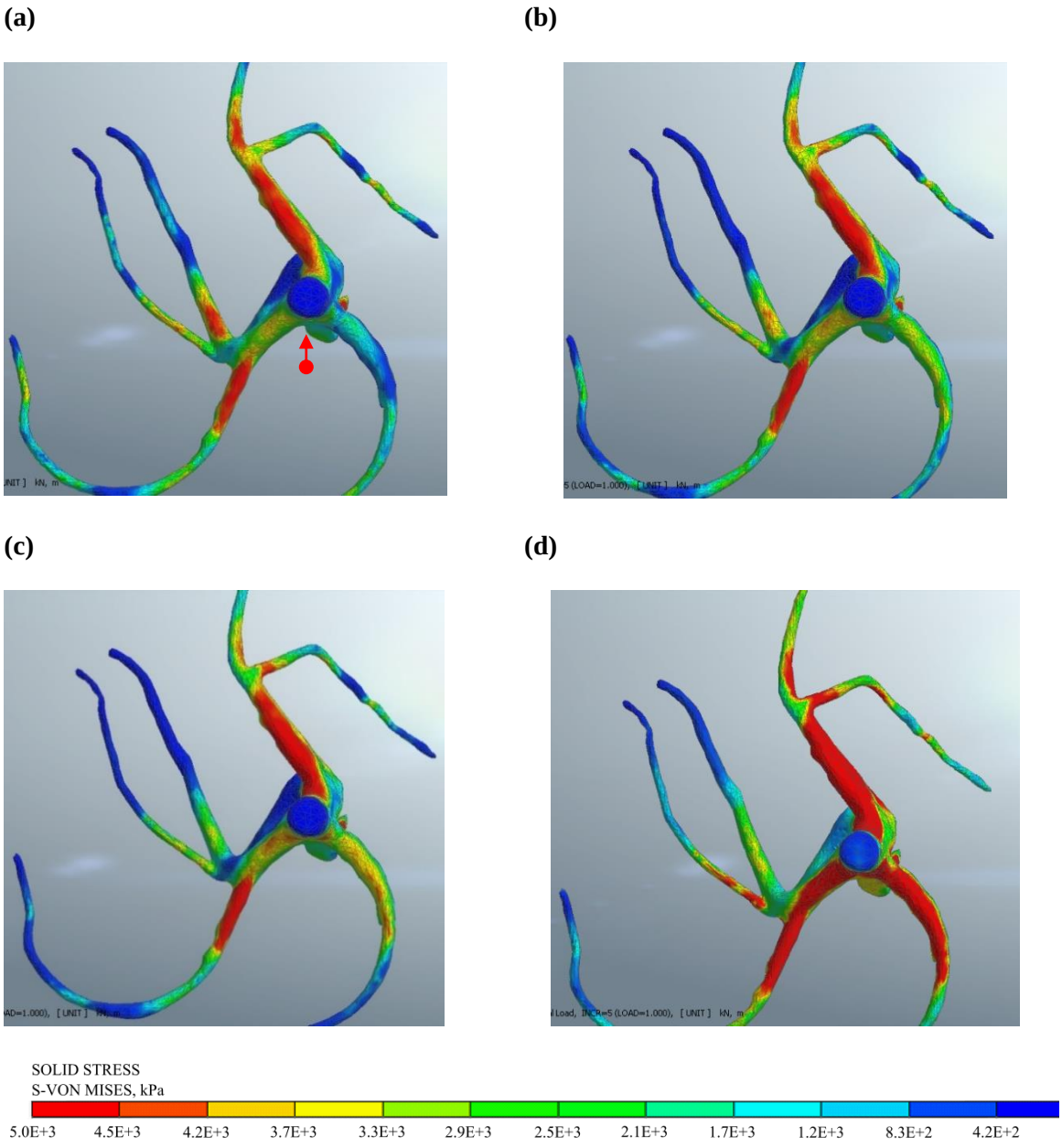

Figure 4-9 Overall stresses of the S. saman tree varying elastic modulus of the soil (a)-Es= 2.5 MPa, (b)- Es= 5.0 MPa, (c)- Es= 10.0 MPa, (d)- Es= 25.0 MPa.

The model for *S. saman* also predicted the dominant contribution of the main roots on the anchorage strength while the secondary roots only developed around 10% of the maximum stresses presented in the main root. For the *S. saman*, the soil-root interaction behaviour also highlighted that an increase in soil rigidity caused the stresses in the base of the trunk to increase especially on the tension side.

According to **Rahardjo et al, (2009)** the elastic modulus of the soil is strongly influenced by the soil type, level of compaction and changes in soil matric suction. The matric suction is in turn also

influenced by climatic conditions, tree canopy leaf area index and soil-water characteristic curve. Using the concept of matric suction and compaction level induced elastic modulus changes, a parametric analysis was conducted by varying the E_{soil} simulating the different soil conditions. The E_{soil} values used are presented in Table 4-1.

Table 4-1 Comparison results obtained from field testing and numerical simulations.

Tree	E_{soil} (MPa)	Overall E (GPa) (Field Load Test)	Overall E (GPa) (Numerical Model)
K. senegalensis	2.5	0.8	0.5
	5.0	-	0.7
	10.0	-	0.8
	25.0	-	1.0
S. saman	2.5	2.0	2.1
	5.0	-	2.7
	10.0	-	3.4
	25.0	-	4.4

4.4 M–α response curves: comparison in-situ behaviour and simulation measurements

Figure 9 shows the relationship between the numerical analyses and the experimental tests for the tree species analysed. The results show a good agreement and highlight the importance of defining an accurate rooting architecture when performing the analysis.

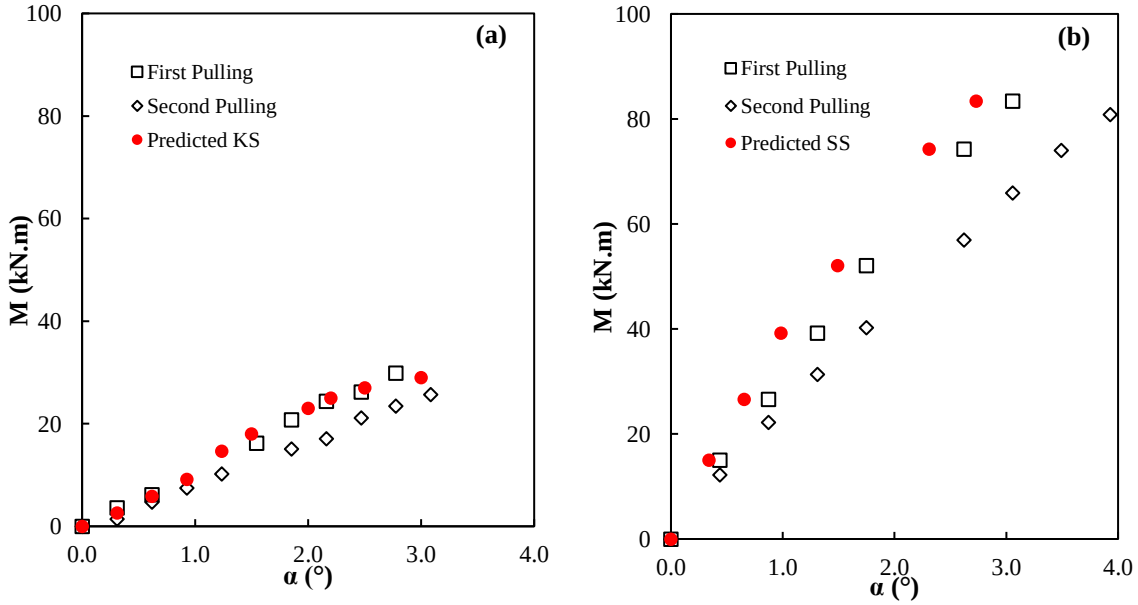

Figure 4-10 Comparison experimental and predicted model, a) *K. senegalensis* (KS), b) *S. saman* (SS).

Within the rotational angle range, the predicted M-α response curves presented in Figure 9 are closer to the field test in terms of magnitude of the bending moment. The predicted values are higher than the ones computed from the static loading test. In general, the maximum overturning forces obtained from the numerical analysis are slightly higher than the measured forces from the field test. This situation can be reasonably explained by the following: i) The simplification of the rooting architecture during the meshing and consequently, an underestimation of the root diameter and lack of higher order rooting architecture ii) the additional deformations due to trunk imperfections and the slings used during the test leading to possible slippages and lower recorded loads/deformations.

The numerical simulations suggest that the contribution of the root on the anchorage strength is strongly affected by the mechanical properties of the soil. However, it is important to note that the simplification of the analysis based on root-plate geometries needs to be improved in terms of rooting preferential paths and soil-root proportion.

4.5 Estimation of structural root protection zone based on actual rooting architecture

For more porous soil profiles, descending roots can penetrate to depths of 1.5–3.0 m (Stone and Kalisz 1991). However, the rooting architectures of the trees air spaded in this study only showed descending root penetration of less than 1.5 m in clean sand. At the same time, the lateral spread was more than 4.0 m. This showed that even within a porous soil like clean sand, the trees growing in the tropical climate of Singapore adapt to the frequent rainfall events and shallow topsoil to possess a shallow and wide spreading rooting system.

Trees can fall in very strong winds, especially if rain has saturated the in-situ soil, reducing the soil strength and moduli of the soil. For Singapore trees, the common rooting system is characterized by shallow rooting depths and consequently, less uprooting resistance due to a shallower mobilized soil depth and thus soil volumes.

One advantage of the numerical model was to allow the evaluation of the mechanical resistance and bonding transfer between the soil and root system. Using numerical modelling, it was possible to estimate the effective length of the roots that provided structural resistance under lateral loading. The threshold value used to define the tree protection zone was the zone of minimum stress concentration, limiting the minimum stress on the tree-roots to 5% of the maximum computed value.

The results presented in Figure 4-11, indicate that the only parts of the entire length of the roots that contribute to the structural resistance. The magnitude of the resistance and the effective root lengths were strongly affected by the soil elastic modulus. In terms of tree-root protection zone (TRPZ), the numerical simulations showed that the TRPZ is within the diameter of the root plate. The TRPZ should be provided for compression and tension side. This is especially true for the case for leaning trees or trees with well-defined canopy centroids.

One relevant finding is that the vertical members of first and second orders of the rooting system that are located close to the main trunk contributed to the tree anchorage and not so much the fine roots. However, further analysis needs to be carried out to validate the contribution of fine roots in the mechanical response. In other analysed scenarios, all the roots only developed stresses depending on the root architecture orientation with relation to the force direction. Similar results regarding the contribution of fine roots to the anchorage strength have been reported by Ji et al. (2018), Yang et al. (2017) and Mickovski (2002).

The numerical model also showed that 30-50% of the length of first order root on the leeward (compression) side contributed to the tree stability while 40-65% length of first order roots the in the windward (tension) side contributed to the tree stability.

Figure 12 presents the stresses obtained from the parametric analysis. It can be observed that the higher stresses were concentrated closer to the trunk and the extension of the effective radius (E_R) moved closer to the trunk when the soil modulus was increased. This reduction in the effective length of the roots with an increase in the elastic modulus of the soil indicated that the effective radius or the estimated root protection zone with reference the axis of the trunk was around 2.5 m for the *S. saman* and 1.5 m for *K. senegalensis*.

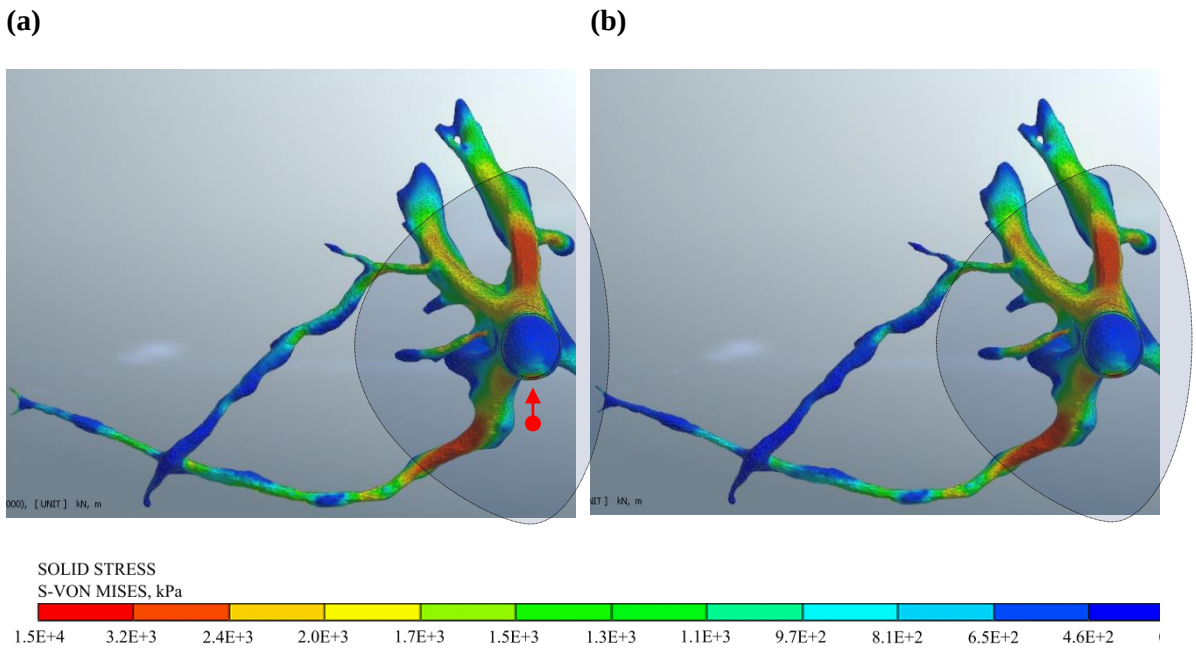

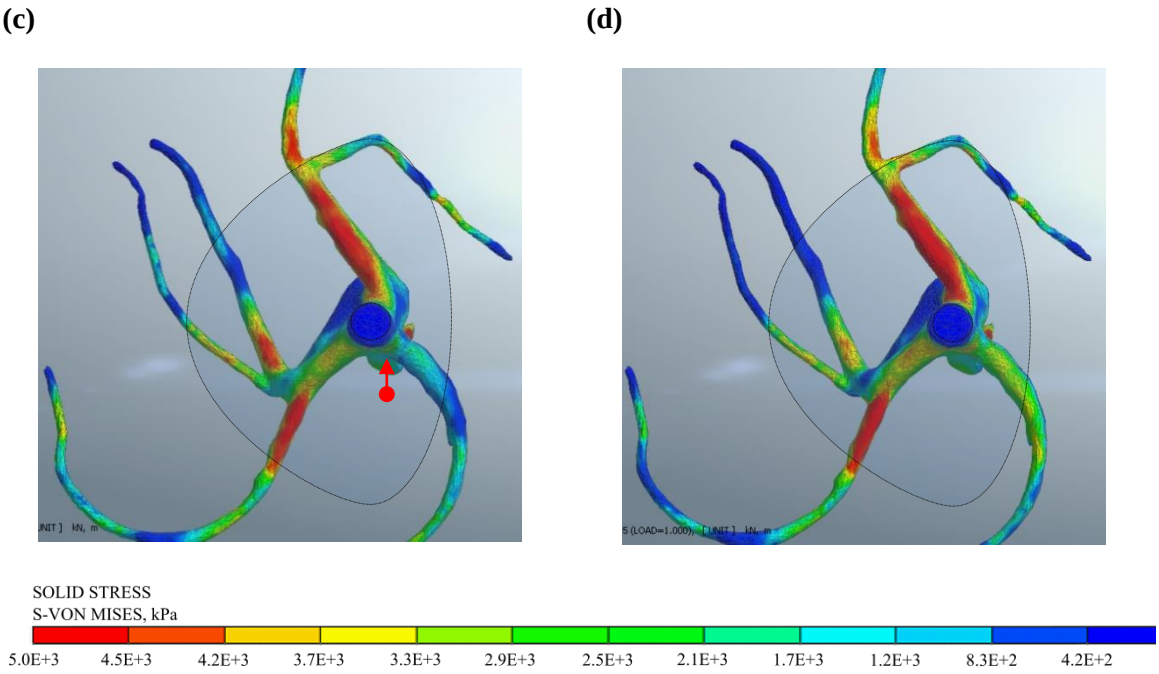

Figure 4-11 Stress contours due to lateral load on root architecture a,b) *K. senegalensis*, c,d) *S. saman*.

4.6 References

- Yang M, Défossez P, Danjon F, Dupont S, Fourcaud T (2017) Which root architectural elements contribute the best to anchorage of Pinus species? Insights from in silico experiments. Plant Soil 411:275–291
- Cannon, J.B., Barrett, M.E., Peterson, C.J., (2015). The effect of species, size, failure mode, and fire-scarring on tree stability. For. Ecol. Manage. 356, 196–203.
- Fourcaud, T., Ji, J.N., Zhang, Z.Q., Stokes, A., (2008). Understanding the impact of root morphology on overturning mechanisms: a modelling approach. Ann. Bot. 101, P1267–1280.
- Lundström, T.; Jonsson, M.J.; Kalberer, M. (2007b) The root-soil system of Norway spruce subjected to turning moment: Resistance as a function of rotation. Plant Soil, 300, 35–49.
- Lundström, T.; Jonas, T.; Stöckli, V.; Ammann, (2007a) W. Anchorage of mature conifers: Resistive turning moment, root-soil plate geometry and root growth orientation. Tree Physiol. 2007b, 27, 1217–1227.
- Nicoll, B.C., Gardiner, B.A., Rayner, B., Peace, A.J., 2006. Anchorage of coniferous trees relation to species, soil type and rooting depth. Can. J. For. Res. 36, 1871–1883.

- Lavers, G.M. (1983). The strength properties of timber. 3rd, revised ed. London (Department Environment. Build. Res. Establishment). 60 p.
- Lee, D. T. -T. (2016). Effect of rainfall on tree stability. Doctoral thesis, Nanyang Technological University, Singapore.
- Dupuy L, Fourcaud T, Lac P, Stokes A. (2007). A generic 3D finite element model of tree anchorage integrating soil mechanics and real root system architecture. American Journal of Botany.; P94:1506–1514.
- Rahardjo H, Harnas FR, Leong EC, et al. (2009) Tree stability in an improved soil to withstand wind loading. Urban for Urban Green 8:237–247
- Stone, E. L., and Kalisz, P. J. (1991). "On the maximum extent of tree roots." Forest Ecology and Management.
- Ji XD, Cong X, Dai XQ, et al. (2018) Studying the mechanical properties of the soil-root interface using the pullout test method. Journal of Mountain Science 15(4). https://doi.org/10.1007/s11629-015-3791-4
- Mickovski (2002). Anchorage mechanics of different types of root systems. Ecology, environment. University of Manchester.

5. CONCLUSION AND REMARKS

5.1 Overall conclusion

This research presents a new model of tree anchorage capable of simulating root breakages for the first time. It also permits the localisation of damage within the root system and includes specific parameterization for root and soil properties based on measurements and experimental evidence reported in the literature. These simulations were performed without any calibration and were found to be in good agreement with the observations. The results are promising enough to envisage further applications to adult trees which are more vulnerable to uprooting than young specimens. However, the architecture of the root system of adult trees is different from that of young trees for P. pinaster. This could increase the degree of complexity of the model.

5.2 Specific Conclusions

In this study, the stress-strain behaviour of three mature trees with different rooting system were analysed by comparing field static load tests and numerical modelling using real rooting architecture. According to the results, it could be concluded that the finite element modelling of the air-spaded roots was able to provide both qualitative descriptions and quantitatively realistic recreations of the static loading tests conducted in the field.

A weaker rooting system with smaller diameter lateral roots will experience higher stresses closer to the modulus of rupture as the soil elastic modulus decreases due to rainfall. Therefore, the ability of the tree to resist bending moments due to lateral loads is influenced by the rooting architecture, the soil properties and climatic conditions.

The numerical modelling showed that the contribution of the structural roots to tree anchorage was primarily dependent on the first order root-morphology that radiates from the trunk face, their orientation and the diameter of the trunk. from moduli variation between 2.5 MPa and Another finding from the numerical modelling was that due to the influence of that the lack of soil strength in tension, the windward root zone undergoing tension was often larger than the leeward (compression) zone.

The tree root studies carried out using MIDAS GTS used actual laser scanned air spaded root architectures simplified into geometries and imported into MIDAS to conduct parametric studies. From the modelling in MIDAS, it was found that the effective root zone is directional in nature for all trees and is larger on the tension side versus the compression of the root plate. The soil stiffness

or modulus played a significant part when the rooting architecture is weaker in terms of lateral root diameters and numbers of lateral roots in line with the lateral load direction.

The parametric studies suggested that the effects of changes in soil elastic moduli strongly affected the overall stiffness of the soil-tree root systems, the stress concentrations and effective rooting area. These changes in E_{soil} can occur because of climatic conditions, soil type, compaction and matric suction changes. Futures studies can consider rainfall induced soil moisture changes and evapotranspiration into the numerical simulations.

In terms of tree-root protection zone (TRPZ), this study shows that there should be a more detailed differentiation of TRPZ needs to be defined according to the windward and leeward side and in terms of the magnitude of the trunk diameter, tree height, canopy size (dripline), estimated rooting depth, soil bulk density and the expected wind speed.

According to the static pull tests the overall stiffness was measured. The preliminary results indicate that the tree overall stiffness is dominated in this order: i) Trunk stiffness, ii) rooting architecture, iii) soil modulus. This method can be adapted to use the measured overall stiffness to assess the tree's anchorage to the soil and thus its stability.

5.3 Future studies

Futures studies may consider the following updates to the present research involving the following recommendations:

- The application of the proposed numerical model can be extended to pursue Pushover analysis based on the derived results.
- Rainfall induced soil moisture changes and evapotranspiration into the numerical simulations.
- Wind-induced changes in the mechanical responses of the tree under different loading directions.
- Effects of drag coefficient on tree stability under dynamic loads.

6. APPENDIX

SPREADSHEET AND NUMERICAL MODEL RESULTS

Table 6-1 Raw data static pulling test

20180807- Static Pulling Test Data												
Geometrical Data												
Average diameter (m)	0.5		**I Tapered (m^4)**	0.0019								
Top perimeter (m)	0.82		**I Circular (m^4)**	0.0031								
Bottom perimeter (m)	1.40											
Tapered ratio (adim)	1.70											
h_m (m)	9.80											
Height Tree (m)												
Rope Length (m)	30.7433											
Strength	7259.4											
Force	7259.4	14518.8	21778.2									
Strain	0.011	0.017	0.027									
Deformation at 1N	4.7E-05	2.5E-05	4.2E-05									
										Tapered section		**Circular Section**
ID	Force (kg)	Normalized Force (kg)	Rope Elongation (cm)	Force (N)	ΔF (kN)	ΔL (m)	Rope deflection (m)	ΔL Normalized Rope deflection (m)	E modulus w/R (GPa)	E modulus R (GPa)	E modulus w/R (GPa)	E modulus R (GPa)
Test 01- Uprooted tree	150	0	0	2943	0	0.00	0.14	0.00	0.0	0.0	0.0	0.0
	163	13	10	3198	0.26	0.05	0.15	0.04	1.5	1.70	4.2	4.7
	210	60	20	4120	1.18	0.10	0.19	0.07	3.5	4.77	2.2	13.3
	236	86	50	4630	1.69	0.25	0.22	0.21	2.0	2.35	1.3	6.6
	245	95	60	4807	1.86	0.30	0.22	0.26	1.8	2.14	1.2	5.9
	253	103	70	4964	2.02	0.35	0.23	0.30	1.7	1.96	1.1	5.5
	264	114	80	5180	2.24	0.40	0.24	0.35	1.6	1.89	1.0	5.3
	279	129	90	5474	2.53	0.45	0.26	0.39	1.7	1.90	1.0	5.3
	289	139	100	5670	2.73	0.50	0.26	0.44	1.6	1.84	1.0	5.1
	306	156	110	6004	3.06	0.55	0.28	0.48	1.6	1.88	1.0	5.2
	311	161	120	6102	3.16	0.60	0.28	0.53	1.5	1.76	1.0	4.9

Table 6-2 Numerical analyses varying the soil elastic modulus of the soil from 2.5 MPa to 10 MPa.

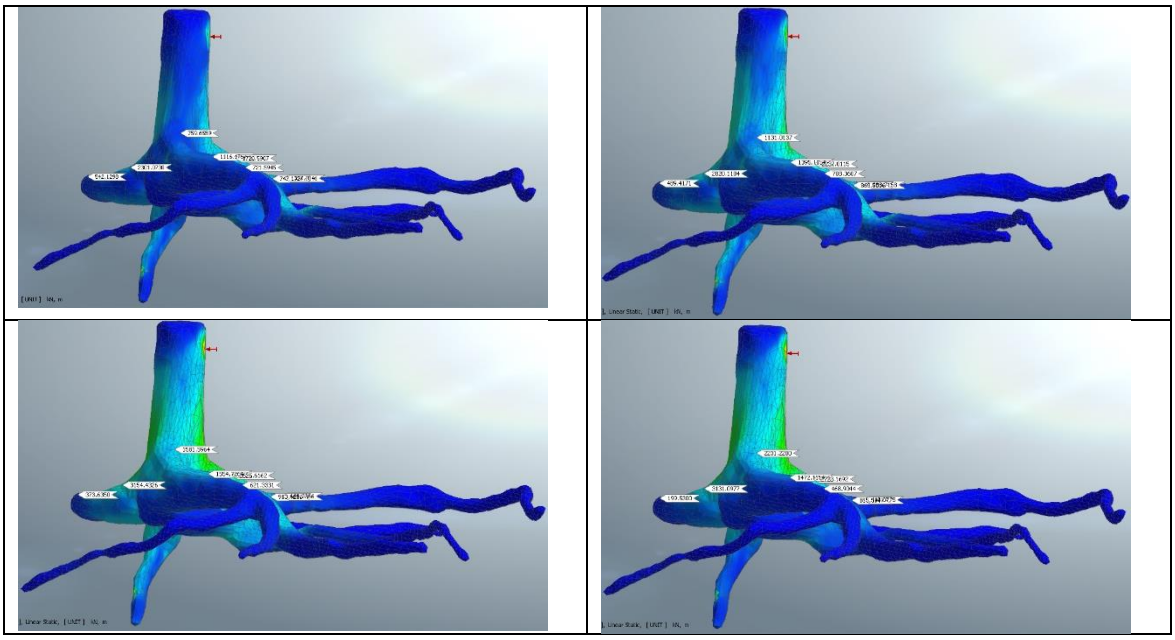

Table 6-3 Numerical analyses varying the loading location